Published paper: Marine and Petroleum Geology 23 (2006) 655-677

Late Ordovician glaciogenic reservoir heterogeneity: an example from the Murzuq Basin, Libya

Daniel Paul Le Heron[a*], Jonathan Craig[b], Owen E. Sutcliffe[c], Robert Whittington[d]

[a]CASP, University of Cambridge, Department of Earth Sciences, West Building, 181A Huntingdon Road, Cambridge, CB30DH.
[b]ENI E&P, V. Emilia, 1, San Donato Milanese, MI, 20097, Italy
[c]Neftex Petroleum Consultants Ltd., 80A Corinthian Court, Milton Park, Abingdon, Oxfordshire, OX14 4RY
[d]IGES, University of Wales, Aberstywtyth, Ceredigion, SY23 3DB

Abstract

In North Africa, Late Ordovician glaciogenic reservoirs account for some c. 3 % of recoverable hydrocarbon reserves, but their heterogeneity and internal complexity means they are poorly understood. To improve this understanding, this paper presents the case study of the Murzuq Basin, SW Libya, and a synthesis of the stratigraphic architecture of Upper Ordovician glaciogenic reservoirs (the Mamuniyat Formation) within it. Particular attention is paid to regionally extensive stratigraphic boundaries and the geometry of sandstone units of potential reservoir quality. Four disconformity-bound units are recognised, the bounding surfaces of which are flat or of high relief. Unit 1 (the oldest) and Unit 3 are mud-dominated and tend towards non-reservoir. In contrast, the Unit 2 and Unit 4 (the youngest) are sand-dominated, have poor to excellent reservoir quality but distinctly different sedimentological architectures across the basin. Unit 2 comprises transitions from glaciofluvial/ intertidal sandstones to offshore turbidites and formed exclusively during glacial retreat. The occurrence of a significant palaeotopography affected sandbody geometry with glaciofluvial/ intertidal deposits concentrating in the lee of these palaeohighs or infilling the bottom of tunnel valleys. Unit 4 is a compound stratigraphic unit recording the effects of glacial retreat and isostatic rebound. In deep marine settings, turbidite fans were deposited during retreat but in shallow water settings, structural reactivation and sediment reworking had a more profound effect on sedimentation. Sedimentological architectures are variable at this level and include prograding coarse clastic wedges (away from a palaeohigh) or the infill of half graben basins during isostatic rebound.

Keywords: Ordovician; Gondwana glaciation; Libya.

1. Introduction

The petroliferous Murzuq Basin occupies some 350,000 km^2 of western Libya and northern Niger (**Fig. 1 A**), and Upper Ordovician (Hirnantian) glacial deposits are the main reservoir targets within this basin. These rocks form part of a Lower Palaeozoic petroleum system that is sourced and sealed by lower Silurian “hot” shale. Until the early 1980s, hydrocarbon systems were unproven within this basin, and exploration was neglected (Hallett, 2002). Approximately 57 wells were drilled between 1958-1997 and almost all intended to test Ordovician prospects (Davidson et al., 2000) with four resulting in large discoveries (including the Elephant and El Shahara fields holding 1-1.5 billion barrels of recoverable liquid reserves) as well as 16 smaller discoveries and 12 wells with shows (Davidson et al., 2000).

A key risk in hydrocarbon exploration is the distribution of the postglacial, organic “hot” shale at the base of the lower Silurian Tanezzuft Formation (Davidson et al., 2000; **Fig. 1 E**). The distribution of this shale, which sources an estimated 90% of Lower Palaeozoic oil in North Africa, is patchy and reflects the residual topography at the upper surface of the Upper Ordovician sediments (Lüning et al., 2000; Lüning et al., 2003). This topography probably results from the combined effects of underfilled palaeovalleys and structures reactivated during isostatic rebound.

Upper Ordovician reservoir rocks are geometrically complex and owe this heterogeneity to deposition under the influence of the West Gondwanan ice sheets (e.g. Sutcliffe et al., 2000a, Ghienne, 2003, Le Heron et al., 2005a). In Libya, the ice sheets repeatedly glacierised the Murzuq Basin and advanced across it towards the NNW (Le Heron et al., 2005). At the prospect scale, individual, subglacially cut palaeovalleys (tunnel valleys) have been described from outcrops on the northern flanks of this basin (Ghienne et al., 2003; Le Heron et al., 2004) and can be compared directly to subsurface, seismically defined examples (e.g. Smart, 2000). Controls on the distribution of these palaeovalleys are not well understood, but may partly reflect the existence of older crustal lineaments (Ghienne et al., 2003).

In the Murzuq Basin, the glaciogenic rocks can be subdivided into four discontinuity-bound architectural units with the best reservoirs primarily in the second and fourth (uppermost) units. Lithostratigraphically, these comprise the Lower and Upper Mamuniyat Members, respectively. In this basin, the number of glacial cycles recognised is controversial, which is due to the differing interpretations of the mud-dominated units (Units 1 and 3 or lithostratigraphically, the Melaz Shuqran Formation and the Middle Mamuniyat Member). These units have been interpreted both as part of a deglacial cycle (Ghienne et al., 2003, el Ghali, 2005) or the deposits of glacial advance (Sutcliffe et al., 2000a, b).

This paper presents new data collected from outcrop analogues from the margins of the Murzuq Basin, giving fresh insights into the depositional controls on Upper Ordovician reservoir heterogeneity. The objective of this work is to provide a synthesis of the stratigraphic architecture of Upper Ordovician glaciogenic reservoirs. In this synthesis, the internal organisation of facies within the sand-dominated, syn-and post-glacial parts of the succession is described in more detail (Units 2 and 4). This paper should also be of interest to geologists interested in the nature of Earth's Ordovician glacial record and its palaeogeographic implications.

1.1 Glaciomarine sedimentation

The occurrence of an ice sheet on a shelf has a profound impact on sedimentation patterns. An ice sheet is both a prolific source of sediment, and has the potential to both create and destroy accommodation space through the effects of isostatic loading, subglacial erosion and post-glacial isostatic rebound. At its maximum, an ice sheet can only extend as far as the shelf break and its patterns of advance and retreat are clearly reflected in the sedimentary record. Glacial successions are separated from one another by a subglacial unconformity (also known as a glacial erosion surface). In areas with significant accommodation space, the deposits of glacial advance comprise large scale, subglacially truncated, progradational units that in vertical section display a distal to proximal transition. Lithologically, the most distal deposits are dominated by mudrocks and fine-grained sandstones, deposited by density currents and ice rafting. The rocks of glacial retreat are commonly organised into a series of geographically isolated, backstepping sandbodies that drape an irregular unconformity (Hambrey et al., 2002). In areas with limited accommodation space, the deposits of glacial retreat may rest directly on a pre-glacial substrate.

Ice sheets display complex patterns of ice flow, and are subdivided into areas of slower and faster moving ice (Dowdeswell and Elverhøi, 2002). Areas of faster flow are referred to as ice streams, which are linear in character, measure up to hundreds of kilometres in length and tens of kilometres in width (Bennett, 2003). These ice streams flow up to ten times faster than the surrounding ice (Bennett, 2003). The effects of these ice streams are significant for hydrocarbon exploration because firstly, they mould, deform and erode the underlying sediments to deposit them mostly in broad palaeogeographical depressions and secondly, they deliver large volumes of sediment to an ice front.

At a smaller scale, glaciated shelves can also modified by anastomosing networks of subglacially formed tunnel valleys filled by the deposits of glacial retreat (and/or subsequent cycles of advance and retreat). These features act as significant conduits for meltwater flow and in North Africa, have produced structures up to several kilometres across and tens to hundreds of metres deep.

2. Study area

This study focusses on the sedimentology and stratigraphy of the Upper Ordovician rocks that outcrop along the northern and western flanks of the Murzuq Basin (**Fig. 1 A-D**). At the western margin (Tihemboka Arch; **Fig. 1 B,C**), these rocks form a continuous outcrop stretching over at least c. 750 km^2, and on the northern flank (Gargaf Arch; **Fig. 1 D**), they crop out over an area of 875 km^2. Two N-S transects were constructed in the Ghat and Wadi Analalin areas of the

Tihemboka Arch (**Figs. 2, 3**), with further W-E and N-S profiles produced for the Gargaf Arch (**Figs. 6, 7**). Together, these data provide a discontinuous proximal-distal profile across 400 km of the Late Ordovician shelf.

LANDSAT images from the study areas were band-ratioed and processed so the colours of the image reflect the clay content of the outcropping lithologies (**Fig. 13**). Shades of blue and yellow indicate a high sand content, whilst shades of magenta are characteristic of mud-rich lithologies. These data were used to map sediment bodies recognised in the field (**Fig. 13**). These include crosscutting tunnel valleys (tens of kilometres long, 4-6 km wide; Ghienne et al., 2003, Le Heron et al., 2004), the pinch-out of the uppermost Ordovician coarse-grained bioturbated progradational wedges (associated with the formation of a warp-like anticline; **Fig. 13**) and extensively developed mega-scale glacial lineations over a 50 X 200 km area (Moreau et al., 2005). Efforts to map out tunnel valleys at outcrop in other regions of North Africa include those of Ghienne and Deynoux (1998) in Mauritania and Beuf et al. (1971) in Algeria. Similar structures have also been recognised in the subsurface of Libya and Algeria (Smart, 2000, Hirst et al., 2002).

3. Geological setting

The Murzuq Basin is flanked by the Tripoli-Tibesti uplift to the east, the Tihemboka Arch to the west, and the Gargaf Arch to the north (**Fig. 1 A**). It has long been supposed that the latter two structures respresented palaeogeographically significant features during the Lower Palaeozoic (Klitzsch, 2000) that were initially generated during the Late Precambrian Panafrican Orogeny. This orogeny involved the accretion of continental and oceanic terranes between the stable West African craton and the Arabian Plate (Coward and Ries, 2003). In western Libya, these processes produced a pronounced NW-SE structural grain (Klitzsch, 2000), with major lineaments (e.g. the 10’30” Fault) regularly re-activated throughout the Lower Palaeozoic (Bellini and Massa, 1980). In the subsurface of the Murzuq Basin, Cambro-Ordovician strata attain 800 m thickness (Davidson et al., 2000), but along the NW-SE trending Mourizidie Horst at the southeastern margins of the basin they are locally thin or even completely absent (Bellini and Massa, 1980; Klitzsch, 2000).

In Libya, Upper Ordovician glaciogenic reservoirs usually rest on the Cambro-Ordovician sandstones and subordinate mudrocks (Radulovic, 1984a,b; Protic, 1984; Gundobin, 1985). These formations include fluvial sandstones of the Upper Cambrian Hassaouna Formation and the bioturbated shallow-marine to intertidal Lower to Mid-Ordovician Ash Shabiyat and Haouaz formations (**Fig. 1 E**). Cambro-Ordovician sandstones are mature to super-mature quartz arenites and record the repeated reworking of sediment in an open, shallow shelf setting with limited accommodation space (Selley, 1997). In the Ghat and Gargaf Arch regions, respectively, the Ash Shabiyat and Haouaz formations form much of the pre-glacial substrate.

In the Murzuq Basin, Upper Ordovician glaciogenic sandstones are onlapped and overlain by the widespread graptolitic shales of the Tanezzuft Formation (**Fig. 1 E**). The age of the earliest-deposited shales is variable and extends from Late Ordovician (*persculptus* Zone) to Aeronian (Lüning et al., 2000). The age variability of the youngest Silurian strata over the basin implies onlap onto a Late Ordovician glacially generated palaeotopography. Regionally, the oldest Rhuddanian shales tend to be organic-rich and potential source rocks (Lüning et al., 2000). At the eastern flank of the Murzuq Basin, in the Mourzidie Horst region, the lowermost Silurian strata onlap Precambrian basement (Klitzsch, 2000) and are sand-dominated (Bellini and Massa, 1980) with poor source potential. The thin nature or absence of Cambro-Ordovician strata at the eastern flank of the Murzuq Basin indicate the existence of significant palaeohighs along the Tripoli-Tibesti Uplift prior to early Silurian transgression.

4. Stratigraphic Architecture

The stratigraphic context of Upper Ordovician glaciogenic reservoirs in Libya is given on **Fig. 1 D**. The regional stratigraphic subdivision/organisation of these strata is shown on the four regional correlation panels (**Figs. 2, 3, 6 & 7**), which are discussed further below. Sedimentological evidence for Late Ordovician ice sheets is now well established and comprises ice-rafted debris, glaciotectonic deformation and the occurrence of subglacially formed tunnel valleys (Sutcliffe et al., 2000; Ghienne et al., 2003; Le Heron et al., 2004; Le Heron et al., 2005; El-ghali, 2005).

The stratigraphic description provided herein should be regarded as an "operational" stratigraphy for the glaciogenic rocks in the Murzuq Basin. This stratigraphy is a hybrid of lithostratigraphy and allostratigraphy and does not necessarily represent a strict, processed-based interpretation of these rocks.

In a review of the upper Ordovician stratigraphy of the Middle East and North Africa, it was suggested that at a continental scale, four main glacial-related allostratigraphic formations could be recognised (Le Heron et al., 2005). The lower three allostratigraphic formations represent true glacial deposits, whilst the youngest characterises both final deglaciation of the shelf and post-glacial tectonism. The oldest allostratigraphic formation is less extensive than those above it and is considered to characterise an initial phase of terrestrial ice-sheet growth (Le Heron et al., 2005). The second and third allostratigraphic formations are more regionally extensive, and represent the growth of a predominantly glaciomarine ice sheet. Units 1-4 of the operationl stratigraphy used here (and described below) are interpreted to correlate with the 2nd, 3rd and 4th allostratigraphic formations (**Fig. 1E**).

4.1 Recognition of stratigraphic units

Four stratigraphic units are identified within Upper Ordovician glaciogenic rocks at outcrop in the Murzuq Basin. These are defined based on five bounding surfaces, meaning that each unit is bounded below and truncated above by a disconformity or angular unconformity. Where angular, unconformities locally display a relief of at least 100 m. The disconformities and unconformities are interpreted as erosion surfaces; in this study, four such surfaces are recognised in ascending stratigraphic position, and are accordingly abbreviated to ES1 (separating the pre-glacial rocks below from the glaciogenic deposits above), ES2, ES3, ES4 and a surface at the base of the post-glacial Tannezuft Formation. Each surface can be traced for tens of kilometres at outcrop along both the western (Tihemboka) and northern (Gargaf) basin margins, areas that are separated by a distance of some 400 km (**Fig. 1 A**). These surfaces are thus regionally extensive. Three of these surfaces- ES2, ES3, and ES4- bear glacially related soft-sediment deformation features, including striated pavements, thrusts, folds and dewatering structures (Le Heron et al., 2005). Each surface was traced with great care on the ground, and checked with the aid of satellite imagery, to ensure that the number of stratigraphic breaks were accurately determined.

However, along strike, units are much more difficult to trace and they are often truncated by overlying units. This lateral variation along strike, which is most pronounced on the Gargaf Arch, reflects the occurrence of large meltwater channels/ tunnel valleys cut on the shelf beneath Late Ordovician ice sheets (Ghienne et al., 2003; Le Heron et al., 2004). Regional palaeogeographic reconstructions of western Libya during the Early Palaeozoic figure a northward-deepening shelf (Selley, 1997), hence the Gargaf Arch would be expected to be along strike from and slightly downdip of the Tihemboka Arch. Between these two regions, units 1 and 3 are easily correlated because they form two distinct mud-prone units. A suite of glacially related deformation structures caps both these units and confirms that these units occur at the same stratigraphic position at both the western and northern basin margins. Regional correlation of these units facilitates a stratigraphic framework and hence interpretation of the sedimentary facies within them. However, for reasons given below, correlation of the sand-dominated units is much more difficult but is possible by the recognition of the same stratigraphic motifs (fining and coarsening upward profiles) in rocks above and below units 1 and 3 at both the western and northern basin margin.

4.2 Palaeotopography on the pre-glacial substrate

Towards the south of Ghat (**Fig. 1 B; Fig. 2 sections A-E**), the pre-glacial Ash Shabiyat Formation is exposed as isolated outliers (or bedrock highs) that define an extensive, but irregular, palaeotopography with a relief of up to 60 m at a major unconformity along erosion surface 1 (ES1). A comparable, several hundred metre deep palaeotopography also occurs on the Gargaf Arch, where a NNE-SSW oriented block of the Haouaz Formation is draped and onlapped to the east, west and north by glaciogenic strata. On seismic sections, a similar palaeotopography is also recognised in the north-central Murzuq Basin in both the Elephant and El Shahara trends (Davidson et al., 2000; McDougall et al., 2004, 2005). Variations in the rugosity of this surface are also apparent because in the Ghat region, this topographic relief appears to be significantly subdued towards the north. These data indicate that the irregular palaeo-relief of ES1 is a widespread phenomenon.

In nearby Iherir, within the Algerian Tassili N'Ajjers plateau (~200 km west of Ghat), similar palaeotopography comprising a network of palaeovalleys up to and >100 m deep is cut onto the "Castellets" member of the In Tahouite Formation (?Upper Ordovician) and filled with the glaciogenic Tamadjert Formation (formerly Unit IV of Beuf et al., 1971). In this region, the palaeotopography is interpreted as being cut beneath ice sheets (Echard et al., 2003). It is unclear whether in the Ghat region topography formed through 1) glacial incision, 2) as lowstand-incised valleys or 3) during local tectonic uplift. Nevertheless, palaeotopography exerts a key influence on glaciogenic reservoir heterogeneity by significantly influencing the distribution of early valley-filling sand, and controlling the overall sediment thickness of the overlying succession.

4.3 Unit 1

Above ES1 in the Tihemboka and Gargaf Arch study areas, Unit 1 comprises a succession lacking coarse sand resting on the basal erosion surface (ES1). In Ghat, the coarsening-upward, muddy and sandy clast-poor diamictite deposits of Unit 1 (sections B & C, **Fig. 2**) locally exceed 60 m in thickness and partly onlap and/or drape palaeotopography on the preglacial substrate. A similar geometrical organisation is noted in the subsurface (Aziz, 2000, McDougall et al., 2005). Prograding clinoforms are also recognised in seismic section (McDougall et al., 2005).

The top of Unit 1 is marked by a major unconformity that is overlain by the sand-dominated deposits of Unit 2. In places, the relief on this unconformity (ES2) is sufficient to reach the preglacial strata (**Fig. 2**, section E). At outcrop on the Gargaf Arch, Ghienne et al. (2003) has described erosion of up to 100 m at ES2 to form a broad palaeotrough that is up to 20 km wide and 60 km long. The margins of these troughs coincide with a faulted or deformed zone affecting pre-glacial deposits and Units 1 to 3.

4.4 Unit 2

In the field, Unit 2 can easily be distinguished from Unit 1 because, as noted above, it is separated from it by a major erosion surface or unconformity (ES2). Below this surface, glacially related soft sediment deformation structures occur, including striated pavements (Section A, **Fig. 2**; Sections M & O, **Fig. 3**; Sections D & F, **Fig. 6**), but also subglacial folds, thrusts and dewatering structures. On the western Gargaf Arch (**Fig. 1 D**), this unconformity is manifested as a 100 m deep, N-S oriented tunnel valley incision. Across the region, between the Ghat and northern Gargaf Arch, Unit 2 is much more sand-dominated than Unit 1 and shows a general northward decrease in grain size away from the palaeohighs (Sections G & H, **Fig. 6**). The basal deposits of Unit 2 locally attain >50 m thickness, are topographically constrained and are typified by medium to coarse-grained sandstones or granule conglomerates (**Fig. 2**, sections A and I, respectively). These traits are not exhibited by the deposits of Unit 1. Sandstones of Unit 2 are significantly coarser than those in Unit 3. In addition, this latter unit is characterised by a higher mud: sand ratio.

On the Gargaf Arch (**Fig. 6**), the basal parts of Unit 2 are truncated by widespread, sheet-like deposit that comprises planar to hummocky or swaley cross-stratified sandstones (Unit 2A). These in turn are capped by a flat but sharp disconformity (ES3, **Fig. 6**). The basal erosion surface of Unit 2A is referred to as ES2A, whilst the uppermost disconformity represents the regionally extensive ES3. Unit 2A is not recognised on the Tihemboka Arch. The reasons for its absence in this region are unclear and require further research. In the subsurface of the Murzuq Basin, an abrupt stratigraphic break is also noted between from Unit 1 (Melaz Shuqran Formation) and Unit 2 (the Lower Mamuniyat member) above (McDougall et al., 2004). In addition, two sandstone packages have also been recognised in Unit 2, with the lowest of these confined to the axes of a palaeovalley and the upper package covering palaeohighs (McDougall et al., 2004). These comparisons indicate that valid ties between outcrop and subsurface data can be achieved.

A suite of soft-sediment deformation structures is also closely associated with the deposition of Unit 2 (Le Heron et al., 2005). On the northern parts of the Gargaf Arch, thrust and fold systems form bands of deformation, extending up to 3 km along strike and 1 km downdip, that include one or more reverse faults or fault tip folds and anticlines of 30 m amplitude. These last structures affect Unit 1 and the basal sandstone of Unit 2. In the central part of the western Gargaf Arch, sediment diapirs measure 30-70 m wide and 20-40 m high, also deforming the basal parts of Unit 2 and Unit 1. These diapirs are clearly onlapped by the laterally extensive sandstones of Unit 2A which conceal the deformation. Sandstones of Unit 2A are largely undeformed but their topmost levels preserve soft-sediment striae (**Fig. 6**, sections C & E).

4.5 Unit 3

In the field, Unit 3 is recognised as a mixed package of sandstone, diamictite and mudrock. It is bounded below by an erosion surface (ES3) on top of unit 2 (or unit 2A on the Gargaf Arch), and above by ES4 which is typically very high relief (~ 100 m). The mud: sand ratio is much higher than underlying deposits of Unit 2 in both the Ghat and Gargaf Arch areas. In this respect, the unit shows some similarities with Unit 1. However, in both the Ghat and Gargaf Arch areas, tracing the rocks at outcrop over tens of kilometres is possible and it is easy to demonstrate that units 1 and 3 are distinct, separate lithosomes. In the latter area, a thin, fining upward motif occurs at the base of this unit that is overlain by the characteristic, thicker, coarsening upward profile. These grain size characteristics may aid distinction of units 1 and 3 in the subsurface of the Murzuq Basin. Towards the west of the Gargaf Arch, a large, branching subglacial tunnel valley was cut into the upper part of this unit and can be mapped at outcrop from LANDSAT images (Ghienne et al., 2003, Le Heron et al., 2004; **Fig. 1 D**). East of this valley, normal faults deform the top of Unit 3 creating half graben. In the subsurface of the Murzuq Basin, Unit 3 (the Middle Mamuniyat member) onlaps and infills the remaining topography at the top of the Haouaz Formation and contains seismically defined clinoforms characteristic of Unit 1. In the Ghat region, Unit 3 is less well exposed but a succession of homogenised diamictites (Section I, **Fig. 2**) thought to represent this unit occurs above stacked, intraformational soft-sediment striated surfaces.

4.6 Unit 4

Recognition and hence regional correlation of Unit 4 hinges heavily upon the identificaton of its lower bounding surface- i.e. ES4- at outcrop in all three outcrops areas, from Ghat, Wadi Analalin and the Gargaf Arch. In the Ghat outcrops, ES4 is the fourth major unconformity to appear in the stratigraphic section from ES1 upwards (**Fig. 2**). Accounting for an additional, transgressive surface at the base of Unit 2A, the same logic is applied to recognise this surface on the Gargaf Arch (**Figs. 6, 7**). In both Ghat and the Gargaf Arch, ES4 forms the highest relief unconformity in the glaciogenic succession. Compared to Unit 3 beneath it, Unit 4 above this unconformity comprises a much higher sand content, and in Ghat, these sands are extensively bioturbated (e.g. section J, **Fig. 2**).

On the Gargaf Arch, basal deposits of Unit 4 infill the tunnel valley cut along ES4. By their very nature, tunnel valleys are local features (incisions are up to several kilometres wide), and thus the following description for the lower part of Unit 4 is a local description and largely follows our earlier work. The basal deposits are comparable with the basal deposits of Unit 2 since they include conglomerates and coarse-grained sandstones. The tunnel valleys are also recognised in seismic section of the Elephant Field (Smart, 2000), 150 km south of outcrops on the Gargaf Arch. These valleys may crosscut/ overlie those identified at the base of Unit 2 and tend to be located further away from the NNW-SSE oriented palaeohigh of the Haouaz Formation (Ghienne et al., 2003). Within the palaeovalleys, a two-part fill is recognised. The lower part, which is locally preserved, includes conglomerates and trough cross-bedded sandstones, interpreted as high energy, ice proximal outwash deposits. These lower rocks are overlain by a more extensive, succession of finer-grained, parallel laminated, hummocky cross-stratified or massive sandstones, organised into a series of backstepping parasequences. These rocks, which are interpreted to record progressive retreat of a glaciomarine ice front, infill, onlap and even overstep the margins of the tunnel valleys (Le Heron et al., 2004). Away from the tunnel valleys, these oldest deposits of Unit 4 are reduced to less than 3 m thick to form a fining upward interval marked at its base by a conglomerate that is positioned above subglacially generated, truncated synclines (Le Heron et al., 2005, fig. 8). These observations compare with those of Unit 2, where sandstones thin over the top of palaeohighs.

Above the base of Unit 4, the nature of the sandstones is highly variable. On the Gargaf Arch, these deposits comprise the fine, current rippled, laminated to hummocky cross-stratified sandstones and siltstones that infill an array of half graben (**Fig. 7**). The thickness of these deposits is strongly influenced by growth faults and folds (see inset, **Fig. 7**). In the Ghat region, rocks of Unit 4 include a succession of coarse-grained to conglomeratic, bioturbated sandstones resting on a prominent and angular unconformity. Well-developed clinoforms prograde away from a palaeohigh (**Figs. 2, 4**). In the Ghat region, the extent of erosion at the base of Unit 4 was sufficient to reach Unit 1 (**Fig. 4**).

In the subsurface of the Murzuq Basin, Unit 4 (the Upper Mamuniyat member) also comprises a stacked and amalgamated succession of sandstones with a lower package of coarse-grained, cross-bedded sandstones that are erosively overlain by a coarsening upward succession of bioturbated, conglomeratic, coarse-grained sandstone (McDougall et al 2004, 2005). These last deposits have well-defined foresets (6º) that infill a palaeotopography at the base of Unit 4.

4.7 Correlations to Wadi Analalin (Fig. 3)

The Late Ordovician glaciogenic rocks of Wadi Analalin comprise thick amalgamated successions of turbidites, which imply sedimentation in a deeper water setting than that of other study areas. This attribute complicates correlation. Units 1 and 4 can be identified with confidence, whilst the separation of Units 2 and 3 is less certain but is attempted herein based on parasequence stacking patterns in these turbidite deposits (**Fig. 3**). A high degree of confidence in correlating Unit 4 between Ghat and Wadi Analalin stems from recognition of the 1) same, high amplitude unconformity beneath it in both regions (ES4) and 2) bioturbation within this unit, which is absent in the underlying succession.

Unit 1 is mud-dominated, coarsens upwards and is capped by the thick, sharp-based amalgamated turbiditic sandstones at the base of Unit 2 (**Figs. 3, 4**). As in the equivalent succession in Ghat, these two units are separated by a distinct unconformity, bearing soft-sediment striae. Above the basal amalgamated sandstones of Unit 2, the glaciogenic deposits are organised into 5 sharp-based parasequences that coarsen upwards from mudrocks to dewatered or laminated turbidite sandstones. The first of these parasequences is thicker than the second, whilst the base of the third is significantly more mud-dominated than those beneath (**Fig. 3**, sections M & N). The base of this muddy parasequence is correlated with the lower part of Unit 3, where backstepping muddy deposits occur both in Ghat (**Fig. 2**, sections I & J) and the Gargaf region (**Fig. 6**, sections B & E). Therefore, in Wadi Analalin, it is proposed that Unit 2 contains the thick and amalgamated sandstones along with the overlying 2 parasequences. Unit 3 comprises the remaining parasequences above up to the bottom of the downcutting and comparatively coarse-grained sandstone of Unit 4 (sections L-O, **Fig. 3**). These are described in more detail below (section 6.1).

4.8 Stratigraphic synthesis

At both the western and northern flanks of the Murzuq Basin, four depositional units are recognised that are bounded at their base by significant discontinuities. By correlating measured stratigraphic sections within and between the Ghat and Wadi Analalin outcrops, a south to north (i.e. landward to basinward) profile across the Tihemboka Arch is presented, covering c. 120 km of this ancient glaciated shelf (**Fig. 4**). Based on these data, a schematic chronostratigraphic chart has been produced (**Fig. 5**) which charts the temporal and spatial development of key reservoir intervals to provide comparison with the subsurface of the Murzuq Basin. In addition, correlation is clearly possible between the northern and western margins of the basin (over a distance of >400 km). Additional erosion surfaces can also be recognised (e.g. at the base of Unit 2A or within Unit 4) but these are less extensive and are not regionally well developed. The origin of the palaeotopography at the base of Unit 1 (ES1) is interpreted to be compound and almost certainly reflects a widespread Ashgill tectonic event, removing much of the preglacial Caradoc to Early Ashgill sequence. However, it cannot be discounted that the initial phase of terrestrial ice sheet-growth could have modified the form of this surface to enhance its rugosity.

Though they contain significant sand content, Units 1 and 3 are significantly muddier than other parts of this glaciogenic succession. For instance, in both the Ghat (sections B & F, **Fig. 2**) and Gargaf Arch (section F, **Fig. 6**) regions, laterally extensive, blanket-like mudrocks onlap onto or drape palaeohighs. The interpretation of these units is equivocal. They may reflect either prograding deposits deposited during glacial advance (Sutcliffe et al., 2000a, b) or blanket mudrock deposition during glacial retreat (Ghienne et al., 2003). The first model is consistent with sediment bodies deposited during glacial advance on Quaternary continental shelves, whilst the latter model bears some comparison to the deglaciation sequences of the Permo-Carboniferous of the Karoo Basin, South Africa (e.g. Visser, 1997).

The interpretation of Unit 2 and the older parts of Unit 4 are less equivocal with a clear development of subglacially formed tunnel valleys. These surfaces represent definite subglacial erosion surfaces, whilst the overlying sandstones were deposited during overall glacial retreat in settings that were ice-proximal becoming more ice-distal up-section. The occurrence of tunnel valleys adds kilometre-scale heterogeneity to the Late Ordovician rocks with additional heterogeneity provided by the development of thrust and fold belts and dome-like folds. These structures represent minor re-advances of an ice front during overall glacial retreat and significantly change the local distribution of sandstones.

On the Gargaf Arch (**Fig. 6**), Unit 2 contains an additional upper sub-unit (Unit 2A). The erosive surface at the base of this sub-unit (ES2A) probably represents the transgressive reworking of ice-proximal sediments. The preservation of soft-sediment striations near to the top of Unit 2A implies that a further readvance of an ice front is likely at this level. On the Gargaf Arch, it was also noted that a wider palaeotrough (up to 20 km wide), preserving thicker successions of Unit 2, was bounded at its margins by syn-sedimentary faults (Ghienne et al., 2003). These data suggest that tectonism continued throughout the Late Ordovician glaciation and had an important influence on the position of depositional thicks and the potential locus of ice streams. Furthermore, these tectonic movements have the potential to allow onlap of Unit 3 onto palaeohighs, creating the valley-like morphologies at the base of this unit.

The nature of Unit 4 is compound with the oldest deposits similar to the glacial retreat sequences of Unit 2. These deposits also infill the tunnel valley that outcrops along the westernmost margin of the Gargaf Arch. After this glacial retreat, the younger deposits of Unit 4 are commonly associated with structural reactivation and/or the localised development of palaeohighs with sedimentation occurring in shallow-marine settings. The deposits are attributed to the reworking of glacial deposits on a post-glacial shelf.

5. Internal facies architecture of syn-glacial sandstones (Unit 2)

On both the Tihemboka and Gargaf arches, Unit 2 represents a widespread, sand-dominated, potential hydrocarbon reservoir that has a variable internal architecture. This variability is described below as an idealised proximal to distal transect but, in reality, parts of this transect may have been removed by later phases of glacial erosion, or through onlap onto bedrock highs. This characterisation builds on the architectural evaluations provided for the Gargaf Arch by Sutcliffe et al (2000a, b), Ghienne et al. (2003) and the basinwide description of lithofacies by el Ghali (2005). Furthermore, McDougall et al (2004, 2005) has also provided architectural information from subsurface data.

5.1 Glaciofluvial to intertidal deposits

These facies are well exposed in Ghat where they rest in high-relief channel-like troughs (>50 m deep and 200 m across) (**Fig. 8 A**) and are characterised by trough cross-bedded sandstones organised into stacked, sharp-based beds, commonly of lenticular geometry. The coarsest sediments occur at the base of these depressions and include very coarse sandstones to matrix-supported conglomerate, with locally preserved inverse grading, intraformational sandstone clasts or flat, discoidal clay chips and sheet-like dewatering structures. These coarse-grained deposits pass vertically and laterally into sigmoidal cross-bedded sandstone with additional current, wave and ladderback ripples. Rain-splash marks also occur (**Fig. 8 B**). Intercalated with these sandstones are parallel laminated, fine to medium sandstones that are cut by decimetric, asymmetrical channels (**Fig. 8 C**). Significant local variation in palaeocurrents occurs, with W, N, NE and SSE-directed dispersal occurring over a small (8 km^2) area.

The occurrence of inverse graded, intraformational conglomerates with sheet-like dewatering structures suggests deposition in part as a subaqueous debris flow that rapidly dewatered upon deposition. Given the context, these debris flows are probably glaciogenic in origin. The sigmoidal cross bedding strongly resembles the tidal megaripple figured in De Vries Klein (1970). The association of these deposits with ladder-back ripples also implies a tidal influence on the deposition of these rocks, which may be responsible for the widely dispersed palaeocurrents in the Ghat region. The occurrence of rain splash marks is consistent with a fluvial or tidally influenced setting where periodic exposure of the sediment surface could have occurred.

On the Gargaf Arch, as in Ghat, the distribution of comparable cross-bedded sandstones is topographically constrained. Here, they rest in the lee of an escarpment of the pre-glacial Haouaz Formation, which coincides with a series of NE-SW to ENE-WSW striking faults. North of this escarpment, ES1 cuts down into Unit 1 (**Fig. 9**). Geometrically, these sandstones form a series of amalgamated lenticular to fan-shaped bodies that reach up to 64 km^2 in area and are cored by coarse-grained sandstone to grain-supported, granular to pebble conglomerates (**Fig. 6, sections G, H**). Grain size decreases laterally towards the margins of these fans but mud-grade sediments rarely occur. Therefore, good porosity and permeability is to be expected in subsurface equivalents.

The fan-shaped geometry of these sediment bodies can be attributed to point-sourced sedimentation from separate meltwater channels. The association of fluvial to intertidal facies with these deposits indictates that these debris flows were reworked by fluvial or tidal processes to form the laterally extensive sandbodies preserved today. One alternative model for the development of these deposits is as the remnants of a line sourced outwash apron that was reworked by transgressive processes during ice sheet retreat (**Fig. 9 C & D**).

5.2 Glaciomarine shelf sand blankets

On the Gargaf Arch, glaciomarine shelf sand blankets form Unit 2A and onlap the underlying intertidal sands (**Fig. 6**). This stratigraphic relationship implies a transgressive relationship between Unit 2A and underlying deposits. The sand blankets are thin (generally <10 m, rarely reaching 20 m), and generally of uniform grain size (fine to medium, well sorted sandstone). These rocks contain parallel laminated sands with parting lineations, stacked and amalgamated swaley cross-stratification (SCS) (**Fig. 10**) and locally preserved trough cross-stratification.

SCS is environmentally diagnostic and is formed by either purely oscillatory, or combined flows in response to storm agitation (Cheel and Leckie, 1993). Therefore, these glaciomarine shelf sand blankets are interpreted as the deposits of an open shelf that was free of sea ice (which can suppress the formation of waves and hence SCS), and that was subject to episodic, very high-energy storms. These shelf sandstones were probably reworked from the recently deposited intertidal sandstones. The clean and reworked character of these deposits suggests that they should have good porosity and permeability. In the subsurface, these deposits will be prone to stratigraphic pinch-out against residual topographic highs.

5.3 Glaciomarine turbidite fans

In Wadi Analalin, Unit 2 comprises a thick and amalgamated succession of turbidites that comprise well exposed, tabular (1-15 m thick) (**Fig. 11 A, C**) or channelised (30 m wide, 10 m thick) (**Fig. 11 B**) sandstone that are interbedded with poorly exposed mudrocks (**Fig. 11 D**). Sandstones are poorly sorted, fine to medium grained, and contain small and randomly oriented clay chips. Petrographic studies demonstrate that they contain an important argillaceous cement of muscovite-sericite-chlorite (Protic, 1984). The tabular beds show sharp to irregular contacts on the underlying mudrocks (**Fig. 3**) with the thicker megabeds (>5m) exhibiting upward transitions from massive to parallel laminated facies. Sheet-like dewatering structures are common within the beds are these are interspersed with horizontal parallel laminae. Thinner sandstone beds (<2-3 m) are parallel laminated and contain convolute laminae and flame structures. In the region of Wadi Analalin, Units 2 and 3 are organised into five coarsening upward parasequences (**Fig. 2**) whose stacking pattern was discussed above.

In Wadi Analalin, these turbidites were deposited on a submarine fan at the foot of a break-in-slope on the continental shelf, and it is suggested that these flows resulted from meltwater outbursts at the ice front. The lateral extent and thickness of the tabular sandstones, together with the significant volume of interstratified mudrocks, implies a very high energy, hydrodynamically efficient turbidite system that was capable of sorting sand from mud (Mutti, 1979) and it is assumed from the coarsening upward character, that these tabular deposits represent sedimentation on a fan-lobe. The channelised deposits are considered to represent the feeder channels. Slope canyon settings can be rejected because of the small scale of incision (<10 m) and the lack of olistostrome and slump deposits. In this setting, the mudrock-dominated interbeds are interpreted as the products of flow lofting as the sands were deposited (e.g. Sparks et al., 1993), together with a component of background sedimentation.

Based on the data presented here, glaciomarine turbidite fans contain a predictable arrangement of potential reservoir sands. These may be likely to yield successful net pays, though the significant argillaceous component in some (Protic, 1984) may mean that primary porosity has been diminished during burial diagenesis. Similar deposits occur within the fill to tunnel valleys in Unit 4 on the Gargaf Arch (Le Heron et al., 2004).

Turbidite depositional processes for these rocks are also the favoured interpretation of Radulovic (1984b). However, one of three main facies associations ("FA4, braided fluvial") recently described by El-ghali (2005) in Wadi Analalin appears to contradict our findings. This author emphasised the importance of trough-cross bedded sand and conglomerate in the interval covered by Unit 2. No such deposits were noted in the course of our study. Nevertheless, despite these differences, El-ghali (2005) considered that lower shoreface-offshore deposits with ice rafted debris (facies association 2), braided fluvial deposits (facies association 4) and lower to upper shoreface deposits (facies association 7) were sufficient to describe Wadi Analalin as one of the "deeper water areas" of the basin. On this point, based on the facies analyis presented herein, we would concur.

6. Internal facies architecture of syn-glacial to postglacial sandstones (Unit 4)

Unit 4 is a transitional stratigraphic unit between the uppermost Ordovician glaciomarine deposits and lowermost Silurian graptolitic shales. Previously, these deposits have been interpreted as the product of post-glacial rebound (Sutcliffe et al., 2000b; el Ghali, 2005) or glacial retreat (Ghienne et al., 2003; Moreau et al., 2005). No previous work has attempted to deal with this conflict of interpretation.

Unit 4 sandstones form some of the key reservoir levels within the Murzuq Basin, particularly in the Elephant and El Sharara fields (Davidson et al., 2000; Aziz, 2000). The nature of the unconformity that separates Unit 4 from Unit 3, and the origin of the residual topography beneath the Lower Silurian graptolitic shales, is also controversial and it is suggested that this surface may be the result of subglacial erosion, post-glacial uplift, post-glacial transgression or a combination of all three processes. It is well known that this topography resulted in "ponds" of anoxia on the post-glacial shelf. Under these anoxic conditions, black shales responsible for 90% of North Africa's Palaeozoic hydrocarbons were deposited (Lüning et al., 2000).

Here, we argue that the deposits of Unit 4 include high-energy glaciomarine sediments deposited during glacial retreat (e.g. the turbidites of Wadi Analalin, described below and the outcropping tunnel valley infills of the Gargaf Arch, Le Heron et al., 2004) or the reworking of glaciomarine strata in post-glacial settings (e.g. in Ghat and half-graben intrabasinal highs on the Gargaf Arch).

6.1 Turbidite sandsheets in Wadi Analalin

As noted above, correlation of units 1-3 between Ghat and Wadi Analalin is difficult (**Fig. 4**), though a well-developed unconformity occurs at the base of Unit 4 (ES4) that displays a basinward shift of sand-dominated facies. Above this surface, the sandstone comprises a thick succession (up to 40 m) of poorly organised and thickly bedded sandstone (**Fig. 3**), which preserves rare intraformational boulders (up to 3 m diameter) (**Fig. 12 A**) set within large-scale, undulose bedforms. Pebble-filled channels and large slumps / recumbent folds also occur within single beds (**Fig. 12 B**). The deposits above and below the slumped sandstones are undeformed. Complex and composite bedforms are also preserved. These include trough and planar cross-beds (commonly amalgamated), current lineated sandstones and climbing sets of unidirectional trough cross bedding (i.e. climbing dunes).

These deposits are interpreted as the product of very high-energy glacial outwash processes deposited during the last phase of glacial retreat. The prevalence of boulders, large bedforms and pebble-plugged channels implies depositional energies far in excess of normal shallow shelf or fluvial high-energy conditions, and are reminiscent of large glacial outbursts (jokülhlaup-type floods, e.g. Carrivick et al., 2004), rather than the normal bedrock-confined braided fluvial deposits of Unit 4 (McDougall and Martin, 2000; el Ghali, 2005). The presence of large-scale slumps may imply a basinward remobilisation of these rapidly deposited sediments. In contrast to the Ghat area, Unit 4 in Wadi Analalin is not associated with a conspicuous uplift or fault structure linked to isostatic rebound.

6.2 Coarse-grained bioturbated sandstone wedges (Ghat)

These rocks form conspicuous conical weathering hills at outcrop, greatly aiding their mapping (**Fig. 14 A**). Approximately 10 km north of Ghat, a NNW-SSE striking, gentle warp-like anticline occurs in the preglacial mudrocks of Unit 1. An angular unconformity (ES4) cuts progressively down into older strata (**Fig. 2**) away from its crest at angles of up to 20° (**Fig. 14 B**). The crest of the anticline is characterised by a very narrow zone (<1.5 km) where the sediments of Unit 4 are not preserved. However, away from the crest, progradational pebbly conglomerate and coarse-grained sandstone, reaching greater than 20 m in thickness occur (**Figs. 10, 11**). In these deposits, a radial palaeocurrent pattern, directed away from the crest of the anticline, is apparent (**Fig. 13**). These sandstones coarsen upwards (**section J; Fig. 2**), but fining upward to homogeneous motifs are also recognised (**sections G, I, K; Fig. 2**). The northernmost deposits are significantly finer-grained than those of the south (**Fig. 13**).

At the base of these sandstones, alternating thinly bedded bioturbated and non-bioturbated sandstones predominate to form well defined, large-scale (>10 m thick), low angle foresets and toesets (**Fig. 14 C**). Vertical and horizontal ichnotaxa are common and include *Diplocraterion*, *Scolithos* and *Thalassanoides*. Each foreset bed is typically massive or fines upwards with a granule lag at the base. Topset units are free of bioturbation and characterised by cross-bedded sandstones filling channels 1.5-2 m deep and 4 m wide (**Fig. 14 D**).

In the Ghat region, the dispersal of palaeocurrents away from the crest of the warp-like anticline implies that this structure acted as a palaeohigh during the deposition of Unit 4. However, the reduced lateral extent of the crestal region (lacking Unit 4) suggests that this area could not possibly have provided all of the sediment deposited in the coarse-grained, bioturbated sandstone wedge.

The unconformity at the base of Unit 4 (ES4) is therefore interpreted as the result of subglacial erosion, which was probably responsible for the differential incision into the mudrocks of Unit 1 (Moreau et al. 2005). During the initial stages of glacial retreat, it is suggested that a series of ice-proximal sandstones were deposited above the surface that were subsequently reworked in a post-glacial marine setting. The northward decrease in grainsize observed within this unit (**Fig. 13**) is compatible with its deposition primarily as an large ice-contact fan, with a retreating ice front depositing the coarsest (most proximal) sediments in the south of the area. However, the coincidence between the palaeocurrent dispersal pattern and a large, warp-like fold in the south of the outcrop area (vicinity of sections I, G: **Fig. 13**) suggests that this ice contact fan was reworked either during or shortly after deposition. Anastomosing fault networks, reflecting heterogeneity in Precambrian basement, crosscut the Tihemboka Arch (Glover, 2000), and there is evidence for major N-S faults in the vicinity that were intermittently active during the Lower Palaeozoic (e.g. the 10°30' fault; Abugares and Ramaekers, 1993). Therefore, it is suggested that the warp-like anticline formed during glacio-isostatic rebound, possibly as a splay of 10°30' fracture system, with a blind fault at depth.

6.3 Half-graben on intrabasinal highs (Gargaf Arch) (Fig. 15, Unit 4)

At approximately the same stratigraphic level as the glacial tunnel valley incisions on ES4 in the westernmost outcrop area of the Gargaf Arch (Ghienne et al., 2003; Le Heron et al., 2004), a series of half graben are preserved in the uppermost sandstones of the Gargaf Arch. These half graben are bounded by steep (60-70°), en echelon normal faults that have a basinward spacing of up to 500m. The area affected by these half graben occurs within a 200 km^2 intrabasinal high (**Fig. 7, Fig. 15 A**). The sandstone infills of these half graben occurs above a high-angle unconformity (ES4) (**Fig. 7**) and shows thickening toward the footwall and multiple, truncated discordances and fault-drag features in the hanging wall (**Fig. 15 B**). Wide zones of ductile deformation separate the half graben: broad, open antiforms with shallowly dipping limbs (<25°) and wavelengths of several hundred metres pass laterally into gentle synclines (**Fig. 15 C**). These wide zones of ductile deformation are most common at the western margin of the intrabasinal high. Beds within the half graben dip N to NE, reflecting growth into S and SW dipping faults, with rare NE-ward dips in the western part of the intrabasinal high (**Fig. 15 A**). Dip orientations are closely comparable to those on the limbs of the broad, open antiforms (**Fig. 15 A**).

The half graben are largely filled by stacked, small-scale (3-7 m), coarsening or thickening-up cycles of silt and sandstone (**Fig. 7**), showing upward transitions from bioturbated and thinly laminated, current or climbing rippled sandstone to massive, thicker, parallel laminated, rippled or trough cross-bedded deposits (**Fig. 16 A**). These coarsening upward cycles comprise massive beds bearing flame and dish and pillar structures, convolute bedding (**Fig. 16 B, C**), and basal flute casts, bounded above and below by minor angular discordances (**Fig. 7**). The topmost sediments in the half graben are erosive and are characterised by bioturbated pebbly sandstone (Sections M & O, **Fig. 7**; **Fig. 16 D, E**), which resembles that of the coarse-grained bioturbated sandstone wedge in Ghat. In these deposits, the cross bedding is oriented to the west and north.

En-echelon half graben and dip data indicate a northeastward sloping sea floor over much of the region covered by half graben, though southwestward dipping faults in the extreme west of the intrabasinal high indicate palaeoslope reversal in this region (see inset, **Fig. 7**, for summary). Glover et al. (2000) interpreted the broad, open antiforms in this western sector to result from compression at the toe of a gravity slide, with upslope extension having formed the half graben. Ghienne et al. (2003) attributed extension to glacioisostatic rebound. On the Gargaf Arch, the geometry of the long wavelength antiforms more closely resembles forced folds that conceal faults at depth (e.g. Withjack et al., 1990) than true contractional structures. This is also supported by the absence of thrust faults.

The prevalence of stacked, coarsening upward cycles suggests that a stick-slip faulting mechanism had a major influence on sediment architecture of half-graben fills (**Fig. 17**). Such an interpretation is compatible with the observation that low angle, laterally restricted discordances bound at least two of the coarsening-upward cycles measured in this study (**Fig. 7**). This model advocates that quiescent sea-floor deposition was periodically interrupted by an influx of sediment due to movement along the half-graben bounding faults and resulting in limited sediment liquefaction (**Fig. 17**). The identification of a stick-slip mechanism within the half graben is significant because sandstones, whilst clean, are thin with multiple pinchouts and lensing geometries and sealed with less prospective mudrocks deposited when faults were inactive.

Two models are proposed for the origins of the half graben (**Fig. 18)**. In the first, a thicker ice cover occupied the intrabasinal high, which upon its recession, resulted in the concentration of glacioisostatic rebound in those areas formerly covered by thick ice (**Fig. 18 A**). Under the second model, a thick ice cover is developed in the westernmost Gargaf Arch, with a thin ice cover further to the east. Thick ice cover in the west resulted in significant glacioisostatic downwarping, laterally displacing the crust, and promoting syn-depositional faulting and the formation of half graben where the ice was thinner (**Fig. 18 B**). This second model is preferred owing to the occurrence of subglacial tunnel valleys, and broader incisions at the base of Unit 2 that may support the occurrence of thicker ice

It is suggested that in the subsurface of the Murzuq Basin, and across the north African region, a universal model for the architecture of the uppermost strata is difficult to apply, because the type and magnitude of glacioisostatic rebound is dependant upon such factors as (i) the degree of crustal depression associated with ice loading, and the thickness of the ice sheet, (ii) the susceptibility of the upper part of the crust to fracture or flexure, which would have been controlled by proximity to major crustal lineaments, (iii) the rate of isostatic uplift, effectively controlling the style of sedimentation, sediment calibre, and energy in the depositional environment (although this is also influenced by the calibre of source sediment), and (iv) the rate of postglacial eustatic sea-level rise over each part of the basin.

7. Conclusions

- Correlation panels constructed for the Tihemboka and Gargaf arches allow a simple stratigraphic model of four architectural units to be recognised. Between these two areas, a correlation framework can be constructed enabling the stratigraphy of 400 km of Late Ordovician shelf to be characterised. The last depositional sequence records final deglaciation of the shelf and was modified by postglacial rebound;
- Detailed description of one depositional sequence (unit 2) shows that:
    1. Ice-proximal, glaciofluvial and intertidal deposits are topographically constrained, relatively clean, and may nucleate in the lee of topographic highs. Locally, these sandbodies have a fan-like geometry, and they were deposited during the initial stages of glacial retreat. These deposits may infill tunnel valleys;
    2. Glaciomarine sand sheets are reworked from the ice-proximal, fluvial and intertidal sandstones but form more laterally extensive, sheet-like bodies. These rocks have a transgressive erosion surface at their base;
    3. Glaciomarine turbidite fans occur in the distal part of a systems tract. They are developed at the base of palaeogeographic intrashelf slopes and are organised into distinctive parasequences. Mudrocks are a common component of this association.
- Unit 4 is compound stratigraphic unit that may possess additional internal erosion surfaces. The oldest deposits of this unit represent glacial retreat and the infill of tunnel valleys. In the more distal part of a systems tract, stacked and amalgamated events accumulate at the base of an intrashelf slope and are potentially derived from large-scale glacial outburst floods;
- In the younger parts of Unit 4, glacial deposits are commonly reworked and redeposited during isostatic rebound. Two distinctive architectures have been identified: 1) half graben depocentres on an intrabasinal high; and 2) coarse grained progradational, bioturbated wedges.

Acknowledgements

Data for this study were collected when DPLeH was in receipt of a PhD studentship funded by the States of Guernsey Education Department (formerly Education Council). LASMO PLC funded the 2001 field season; Agip North Africa B.V funded the 2002 field seasons. Khalid Bergig, Juma Mayouf and Hesham Benshatti from PRC are thanked for their excellent support in the field. This article was written in CASP, Cambridge University, where colleagues are kindly acknowledged for their support and encouragement during the drafting of this work. The manuscript benefited from the thorough and constructive external reviews of Dr Bruce Levell and Dr Pieter Spaak (Shell), Dr David Hinds (Exxon), and an internal review by Dr Robert Scott (CASP). Professor David Roberts is thankfully acknowledged for his editorial work on the manuscript.

References

Abugares, Y.I., Ramaekers, P., 1993. Short notes and guidebook on the Palaeozoic Geology of the Ghat area, SW Libya. Earth Science Society of Libya- Sedimentary Basins of Libya (First Symposium). Sirte Oil Company.

Anfray, R., Rubino, J.L., 2003. Shelf Depositional Systems of the Ordovician Hawaz Formation in the Central Al Qarqaf High. In: Salem, M.J., Oun, K.M. (Eds.). Geology of Northwest Libya, vol. II. Earth Science Society of Libya/ Gutenburg Press, Malta. 19-34.

Aziz, A., 2000. Stratigraphy and hydrocarbon potential of the lower Palaeozoic succession of licence NC115, Murzuq Basin, SW Libya. In: Sola, M.A. and Worsley, D. (Eds.), Geological Exploration of the Murzuq Basin. Elsevier, Amsterdam, 485-509.

Bellini, E., Massa, D., 1980. A stratigraphic contribution to the Paleozoic of the southern basins of Libya. In: Salem, M.J. & Busrewil, M.T. (Eds.) The Geology of Libya I. Academic Press, London, 3-56.

Bennett, M.R., 2003. Ice streams as the arteries of an ice sheet: their mechanics, stability and significance. Earth Science Reviews 61 (3–4), 309–339.

Beuf, S., Biju-Duval, B., de Charpal, O., Rognon, P., Gariel, O., Bennacef, A., 1971. Les Gres du Palaeozoique inferieur au Sahara. Editions Technip, Paris. 464 pp.

Carrivick, J.L., Russell, A.J., Tweed, F.S., 2004. Sedimentology and palaeohydrology of jökulhlaups from Kverkfjöll, Iceland. Sedimentary Geology 172, 19-40.

Cheel, R.J., Leckie, D.A., 1993. Hummocky cross-stratification. Sedimentology Review, 103-122.

Coward, M. P., Ries, A. C., 2003. Tectonic development of North African basins. In: Arthur, T., Macgregor, D. S., Cameron, N. R. (Eds.). Petroleum Geology of Africa: New Themes and Developing Technologies. Geological Society, London, Special Publication 207, 61-84.

Davidson, L., Beswetherick, S., Craig, J., Eales, M., Fisher, A., Himmali, A., Jho, J., Mejrab, B., Smart, J., 2000. The structure, stratigraphy and petroleum geology of the Murzuq Basin, southwest Libya. In: Sola, M.A., Worsley, D. (Eds.), Geological Exploration of the Murzuq Basin. Elsevier, Amsterdam, 295-320.

De Vries Klein, G., 1970. Depositional and dispersal dynamics of intertidal sand bars. Journal of Sedimentary Petrology 40, 1095-1127.

Dowdeswell, J.A. and Elverhøi, A, 2002, The timing of initiation of fast-flowing ice streams during a glacial cycle inferred from glacimarine sedimentation. Marine Geology, 188, 3-14.

Eschard, R., Abdallah, H., Braik, F., Desaubliaux, G., 2003. Lower Palaeozoic Sedimentation in the Tassili N’Ajjer, Algeria. Fieldguide to the AAPG Hedberg Conference (Algiers) Field Trip. SONATRACH-IFP publication, 103p.

El ghali, M.A.K., 2005. Depositional environments and sequence stratigraphy of paralic glacial, paraglacial and postglacial Upper Ordovician siliciclastic deposits in the Murzuq Basin, SW Libya. Sedimentary Geology 177, 145-173.

Ghienne, J-F., 2003. Late Ordovician sedimentary environments, glacial cycles, and post-glacial transgression in the Taoudeni Basin, West Africa. Palaeogeography, Palaeoclimatology, Palaeoecology 189, 117-145.

Ghienne, J-F., Deynoux, M., 1998. Large-scale channel fill structures in Late Ordovician glacial deposits in Mauritania, western Sahara. Sedimentary Geology 119, 141-159.

Ghienne, J-F., Deynoux, M., Manatschal, G., Rubino, J-L., 2003. Palaeovalleys and fault-controlled depocentres in the Late-Ordovician glacial record of the Murzuq Basin (central Libya). Comptes Rendus Geosciences 335, 1091-1100.

Glover, T., 2000. Aspects of Deformation in Saharan Intracratonic Basins. PhD thesis, University of Wales, Aberystwyth.

Glover, T., Adamson, K., Whittington, R., Fitches, W., Craig, J., 2000. Evidence for soft sediment deformation- the Duwaysah Slide of the Gargaf Arch, central Libya. In: Sola, M.A., Worsley, D. (Eds.). Geological Exploration of the Murzuq Basin. Elsevier, Amsterdam, 417-447.

Gundobin, V.N., 1985. Geological Map of Libya Sheet NH-33 (Qararat al Marar) and Explanatory Booklet. Industrial Research Centre, Tripoli.

Hallett, D., 2002. Petroleum Geology of Libya. Elsevier, 508p.

Hambrey, M.J., Barrett, P.J., Powell, R.D., 2002. Late Oligocene and early Miocene glacimarine sedimentation in the SW Ross Sea, Antarctica: the record of offshore drilling. In: Dowdeswell, J.A. and O Cofaigh, C. (eds) Glacier-Influenced Sedimentation on High-Latitude Continental Margins, Geological Socity Special Publications, 203, 105-128.

Hirst, J.P.P; Benbakir, A., Payne, D.F., Westlake, I.R., 2002. Tunnel Valleys and Density Flow Processes in the upper Ordovician glacial succession, Illizi Basin, Algeria: influence on reservoir quality. Journal of Petroleum Geology 25, 297-324.

Klitzsch, E., 2000. The structural development of the Murzuq and Kufra basins- significance for oil and mineral exploration. In: Sola, M.A., Worsley, D. (Eds.). Geological Exploration of the Murzuq Basin. Elsevier, Amsterdam, 143-150.

Le Heron, D., Sutcliffe, O., Bourgig, K., Craig, J., Visentin, C., Whittington, R., 2004. Sedimentary architecture of Upper Ordovician tunnel valleys, Gargaf Arch, Libya: Implications for the genesis of a hydrocarbon reservoir. GeoArabia 9, 137-160.

Le Heron, D.P., Sutcliffe, O.E., Whittington, R.J., Craig, J., 2005. The origins of glacially related soft-sediment deformation structures in Upper Ordovician glaciogenic rocks: implication for ice sheet dynamics. Palaeogeography, Palaeoclimatology, Palaeoecology 218, 75-103.

Lüning, S., Craig, J., Loydell, D.K., Storch, P., Fitches, W., 2000. Lowermost Silurian "hot shales" in north Africa and Arabia: regional distribution and depositional model. Earth Science Reviews 49, 121-200.

Lüning, S., Kolonic, S., Loydell, D.K., Craig, J., 2003. Reconstruction of the original organic richness in weathered Silurian shale outcrops (Murzuq and Kufra basins, southern Libya). GeoArabia 8, 299-308.

McDougall, N., Martin, M., 2000. Facies models and sequence stratigraphy of Upper Ordovician outcrops of the Murzuq Basin, SW Libya. In: Sola, M.A., Worsley, D. (Eds.). Geological Exploration of the Murzuq Basin. Elsevier, Amsterdam, 223-236.

McDougall, N.D., Clarke, P., Fitches, W.R., McDonnell, A., Mokhtari, N., Hussein, A., 2003. Glaciers and Grabens: the origins of palaeovalleys in the Tamadjert Formation (Unit IV) of the Algerian Sahara. In American Association of Petroleum Geologists Hedburg Conference: Palaeozoic and Triassic Petroleum Systems in North Africa- abstract volume.

McDougall, N.D., Tawengi, K., Quin, J.G., Vila Pont, J., Tur Fernandez, N., Garcia Victoria, E., Martin, J.J., Pena Forero, J., 2004. From outcrop to seismic: the Upper Ordovician of the Murzuq Basin, SW Libya (Melaz Shuqran and Mamuniyat Formations), an example of intrgrated seismic, well and outcrop data, 3rd PESGB/HGS International Conference on Africa E & P, Abstract volume, 160-168.

McDougall, N.D., Tawengi, K., Quin, J., Vipla Pont, J., 2005. Depositional environments and large-scale sediment architecture in the Upper Ordovician of the Murzuq Basin, SW Libya (Melaz Shuqran and Mamuniyat Formations, EAGE, 2nd North African/Mediterranean Petroleum and Geoscience Conference, Abstract volume, 8.

Moreau, J., Ghienne, J-F., Le Heron, D.P., Rubino, J-L., Deynoux, M., 2005. A 440 Million year old ice stream in North Africa. Geology 33 (9), 753-756.

Mutti, E., 1979. Turbidites et cones sous-marine profonds. In: Homewood, P. (Ed.) Sedimentation detritique (Fluviatile, Littorale et Marine), Institut de Geologie, Universite de Fribourg, 353-419.

Protic, D., 1984. Geological Map of Libya- Sheet NG 32-7 (Tikimuit Sheet) and Explanatory Booklet. Industrial Research Centre, Tripoli.

Radulovic, P., 1984a. Geological Map of Libya- Sheet NG 32-11 (Tannezuft Sheet) and Explanatory Booklet. Industrial Research Centre, Tripoli.

Radulovic, P., 1984b.Geological Map of Libya- Sheet NG 32-15 (Ghat Sheet) and Explanatory Booklet. Industrial Research Centre, Tripoli.

Selley, R.C., 1997. The Sedimentary Basins of NW Africa: Stratigraphy and Sedimentation. In: Selley, R.C. (Ed.). African Basins, Sedimentary Basins of the World 3. Elsevier, Amsterdam, 3-16.

Smart, J., 2000. Seismic expressions of depositional processes in the upper Ordovician succession of the Murzuq Basin, SW Libya. In: Sola, M.A.,Worsely, D. (Eds.). Geological Exploration of the Murzuq Basin. Elsevier, Amsterdam, 397-415.

Sparks, R.D.J., Bonnecaze, R.T., Huppert, H.E., Lister, J.R., Hallworh, M.A., Mader, H., Phillips, J. 1993. Sediment-laden gravity currents with reversing buoyancy. Earth and Planetary Science Letters 114, 243-257.

Sutcliffe, O.E., Adamson, K. & Ben Rahuma, M.M., 2000a. The Geological Evolution of the Palaeozoic Rocks of Western Libya: A Review and Fieldguide. Earth Science Society of Libya (ESSL), Tripoli.

Sutcliffe, O.E., Dowdeswell, J.A., Whittington, R.J., Theron, J.N., Craig, J., 2000b. Calibrating the Late Ordovician glaciation and mass extinction by the eccentricity cycles of the Earth's orbit. Geology 23, 967-970.

Visser, J.N.J., 1997. Deglaciation sequences in the Permo–Carboniferous Karoo and Kalahari basins of southern Africa: A tool in the analysis of cyclic glaciomarine basin fills. Sedimentology 44, 507–521

Withjack, M.O., Olson, J., Peterson, E. 1990. Experimental models of extensional forced folds. American Association of Petroleum Geologists Bulletin 74, 1038-1054.

Figure captions

Figure 1 A: The main basement, Cambro-Ordovician and Silurian outcrops in Libya around the flanks of the Murzuq and Kufra basins. In this study, architectural models developed at outcrop from the flanks of the Murzuq Basin (maps B, C, D) should have direct relevance to exploration in both basins. Maps B, C and D show both the location of measured sections and transect orientations shown in Figs. 2-4. Geological maps are derived from previous authors, and subdivide Late Ordovician glaciogenic rocks into Melaz Shuqran Formation and an overlying Mamuniyat Formation for most of the Murzuq Basin (Protic (1984) recognises an additional Tasghart Formation between these two units in Wadi Analalin. B: Map for Ghat (S Tihemboka Arch), with surface geology after Radulovic (1984b). C: Map for Wadi Analalin (N Tihemboka Arch), with surface geology after Protic (1984). D: Map for the Gargaf Arch, with surface geology modified slightly after Gundobin (1985). E: Stratigraphic column showing position of the Late Ordovician glaciogenic reservoirs within the stratigraphy of the Murzuq Basin.

Figure 2 Correlation panel constructed from outcrops of Upper Ordovician glaciogenic strata in the Ghat region, Tihemboka Arch. For location, see Fig. 1 B. Co-ordinates of each of the logged sections are as follows. A) 24°52.021'N 010°10.861'E; B) 24°53.719'N 010°09.824'E; C) 24°55.755'N 010°11.078'E; D) 24°57.935'N 010°10.925'E (Ghat Fort); E) 25°01.522'N 010°08.154'E; G) 25°02.140'N 010°05.606'E; H) 28°13.859'N 012°48.243'E; I) Composite log constructed from 3 localities- (i) 25°04.628'N 010°07.650'E, (ii) 25°04.922'N 010°08.031'E, (iii) 25°05.056'N 010°08.210'E; J) 25°04.064'N 010°03.471'E; K) 25°04.985'N 010°03.497'E.

Figure 3 Correlation panel constructed from outcrops of Upper Ordovician glaciogenic strata in the Wadi Analalin region, Tihemboka Arch. For location, see Fig. 1 C. For legend, see Fig. 2. In this area, the sedimentological signature of units 2-3 (well developed in Ghat) is encrypted within five locally developed parasequences, which occur above stacked turbidites at the base of Unit 2. Glacial outburst flood deposition (jokulhlaup deposits) is the preferred interpretation for Unit 4. The glacial erosion surface beneath these rocks (ES4) signifies one of the most significant phases of glacial advance across the basin. Co-ordinates of each of the logged sections are as follows: L) 25°54.122'N 009°55.445'E; M) 26°00.382'N 009°53.213'E; N) 26°04.601'N 009°52.350'E; O) 26°04.798'N 009°47.710'E.

Figure 4 Sketch showing interpreted architecture of Late Ordovician glaciogenic rocks on the Tihemboka Arch based on figures 2 and 3. The sketch enables a 120 km proximal-distal (left to right) transect of the shelf to be characterised in detail. Note regional development of ES4 and Unit 4 above it.

Figure 5 Chronostratigraphic framework for Late Ordovician glaciogenic rocks in Libya based upon the sections correlated between Ghat to Wadi Analalin. This framework very clearly identifies 4 depositional units. During the fourth cycle and final retreat of the ice sheets, a key reservoir interval (Unit 4) was deposited. This unit is composite in nature. The earliest deposited sediments are interpreted to record final deglaciation of the basin (in Wadi Analalin); later deposited sediments (in Ghat) were reworked by glacioisostatic rebound processes.

Figure 6 A: South-to-north oriented correlation panel across the Gargaf Arch (location shown in Fig. 1 D); correlation is relatively straightforward despite crosscutting palaeovalleys occurring at right angles to this transect. A similar stratigraphic subdivision to that in the Tihemboka Arch is proposed. The key difference is that unit 2 has a separate subunit at its top (Unit 2A). Co-ordinates of each of the logged sections are as follows. A) 27°36.707'N 012°52.064'E; B) 27°39.656'N 012°49.785'E; C) Gara Antelope, Mamuniyat Formation type section; D) 27°46.174'N 012°49.323'E; E) 27°46.785'N 012°47.869'E; F) 27°56.433'N 012°43.499'E; G) 28°07.437'N 012°44.820'E; H) 28°09.156'N 012°45.482'E; I) 27°36.707'N 012°52.064'E; J) 28°20.126'N 012°53.597'E; K) 28°21.347'N 012°52.338'E; L) 28°21.827'N 012°51.477'E.

Figure 7 Correlation panel across the intrabasinal high on the western Gargaf Arch affected by half-graben faulting (location shown in Fig. 1 D). Sediments within this basin are almost entirely restricted to Unit 4 and the profile of individual measured sections is strongly dependant on their position relative to half-graben or warp-like folds (see inset sketch). The characteristic motif of sediments is a punctuated coarsening-up profile, thought to reflect stick-slip faulting during subsidence (see Fig. 17).

Figure 8 Characteristic features of glaciofluvial and intertidal deposits in Ghat. A: Large incision (possibly an enormous ice carved groove) containing stacked, coarse-grained glaciofluvial sandstone (Unit 2, section B, Fig. 2). B: Exquisitely preserved rainsplash marks, testament to periodic emergence in a terrestrial or intertidal setting (Unit 2, section C, Fig. 2). C: Asymmetric channels cutting into planar bedded sandstones (Unit 2, section F, Fig. 2).

Figure 9 Two equally plausible models explaining the disconnected nature of glaciofluvial deposits within Unit 2, developed for the northern Gargaf Arch. Model 1 suggests that a fan-like geometry could be achieved by the formation of point-sourced ice contact fans, whereas model 2 emphasises that similar geometries could be achieved through reworking of a more line-sourced system during ice sheet recession.

Figure 10 Characteristic low-angle swaley cross-stratification developed in a glaciomarine sand blanket, Unit 2A, Gargaf Arch (section G, Fig. 6).

Figure 11 Turbidite lithofacies in Wadi Analalin. These were probably deposited at the foot of a minor slope on the continental shelf. Units 2-3 are difficult to differentiate in this area. Locally persistant parasequences are identified (A), and the lateral extent of wedge-shaped (overbank) turbidites is clearly apparent from this photograph (geologist circled for scale). B: Channelised turbidites. Landcruiser (approximately 50 m from outcrop) for scale. C: Thicknesses of individual turbidite sandstone beds can exceed 15 m, leading to the prospect of vertically stacked pays. D: Small coarsening upward cycle (parasequence 5) comprising mudrock above a thick sandstone bed.

Figure 12 A: Example of very large boulders that are preserved within coarse-grained sandstone to granule conglomerates in Unit 4, Wadi Analalin (section L, 37 m, Fig. 3). These deposits, occur above the base of Unit 4 and are interpreted as the products of jokulhlaups, or glacial meltwater outburst floods. B: Large-scale soft-sediment deformation (recumbent folds) in Unit 4, Wadi Analalin (section O, 52-59 m, Fig. 3).

Figure 13: $LANDSAT_{TM}$ data covering the Ghat region. The southern part of the image shows mega-scale glacial lineations, part of a dataset that identified the "footprint" of an ancient ice stream (Moreau et al., 2005). The northern part of the image shows the lateral distribution of the coarse-grained bioturbated sandstone wedge of unit 4, a major reservoir target beneath the hot shale (this shale is picked out clearly in red). This wedge was deposited above a high-angle unconformity during the final phase of glacial retreat. The rose diagrams clearly show how this sand sheet was reworked during uplift (rebound), but the narrow area of non-exposure (?erosion) north of section F relative to the size of the area over which this sand is distributed demonstrates that it did not provide the principal sediment source, which is ascribed to the last phase of glaciation to affect Ghat and the Tihemboka Arch. Bands were subject to histogram stretching, directional/ "sunlight" filtering and, most importantly, band-ratioing using combinations of bands 1, 4, and 7. The $LANDSAT_{TM}$ image attempts to emphasise clay content at outcrop. Purple hues indicate mud-dominated deposits, and blue/ cyan hues more sandy sediments. Bright yellows and greens are a good indication of the distribution of sandy (both ancient and modern) sediment.

Figure 14 A: General view of the coarse-grained bioturbated sandstone wedge of Unit 4, Ghat. Clay contents are low and typical conical weathering character is attributable to an evenly spaced jointing pattern. B: Illustration of subglacial unconformity ES4 at the base of Unit 4, Ghat. C: Bipartite subdivision of the coarse-grained sandsheet, Unit 4, Ghat recognising bottomset and foreset units. D: Channel fill deposits, typical of topsets within this sandstone.

Figure 15: Forced folds and growth faults- typical structural elements of the fault-bounded half graben on the Gargaf Arch. A: Dip data collected from half-graben (marked “H” in the centre of each stereogram) and the limbs of warp-like folds (marked “F” in the centre of each stereogram). Arrowheads denote principal orientation of compression or extension. The figure contains data from localities additional to the logged sections in Fig. 7; these are asterisked. Co-ordinates of each of the localities shown are as follows: A) 27°41.686’N 012°48.579’E; B) 27°41.758’N 012°45.804’E; C) 27°42.534’N 012°43.875’E; D) 27°40.295’N 012°44.645’E; E) 27°47.203’N 012°42.473’E; F) 27°38.083’N 12°43.950’E; G) 27°39.165’N 12°44.873’E; H) 27°41.474’N 012°45.105’E. B: Example of en-echelon half graben array; each half graben is characterised by extensive growth and drag in the hanging wall. C: Photo and sketch showing geometry of warp-like folds and their relation to faults in the mini-basin.

Figure 16: Typical facies within the half graben on the Gargaf Arch. Facies reflect calm, low energy shallow marine conditions punctuated by the influx of gravity flow deposits. These variations are attributed to alternating periods of quiescence and activity along half-graben bounding faults. A: Stacked interference ripples. B: Flame structures. C: Convolute bedding (pen tip bottom-centre of photo for scale). D: Large, isolated vertical burrow. E: Bioturbated sandstone bed at top of the succession.

Figure 17: Model for generating punctuated coarsening/thickening up cycles driven by a stick-slip mechanism along half-graben bounding faults, Gargaf Arch.

Figure 18: Two alternative models for the formation of half graben at the margins of tunnel valleys. A: Glacioisostatic loading under an unevenly distributed ice sheet load and B: post-glacial isostatic

rebound. The first model (glacioisostatic depression) is preferred owing to the occurrence of tunnel valleys at the same stratigraphic level to the west.

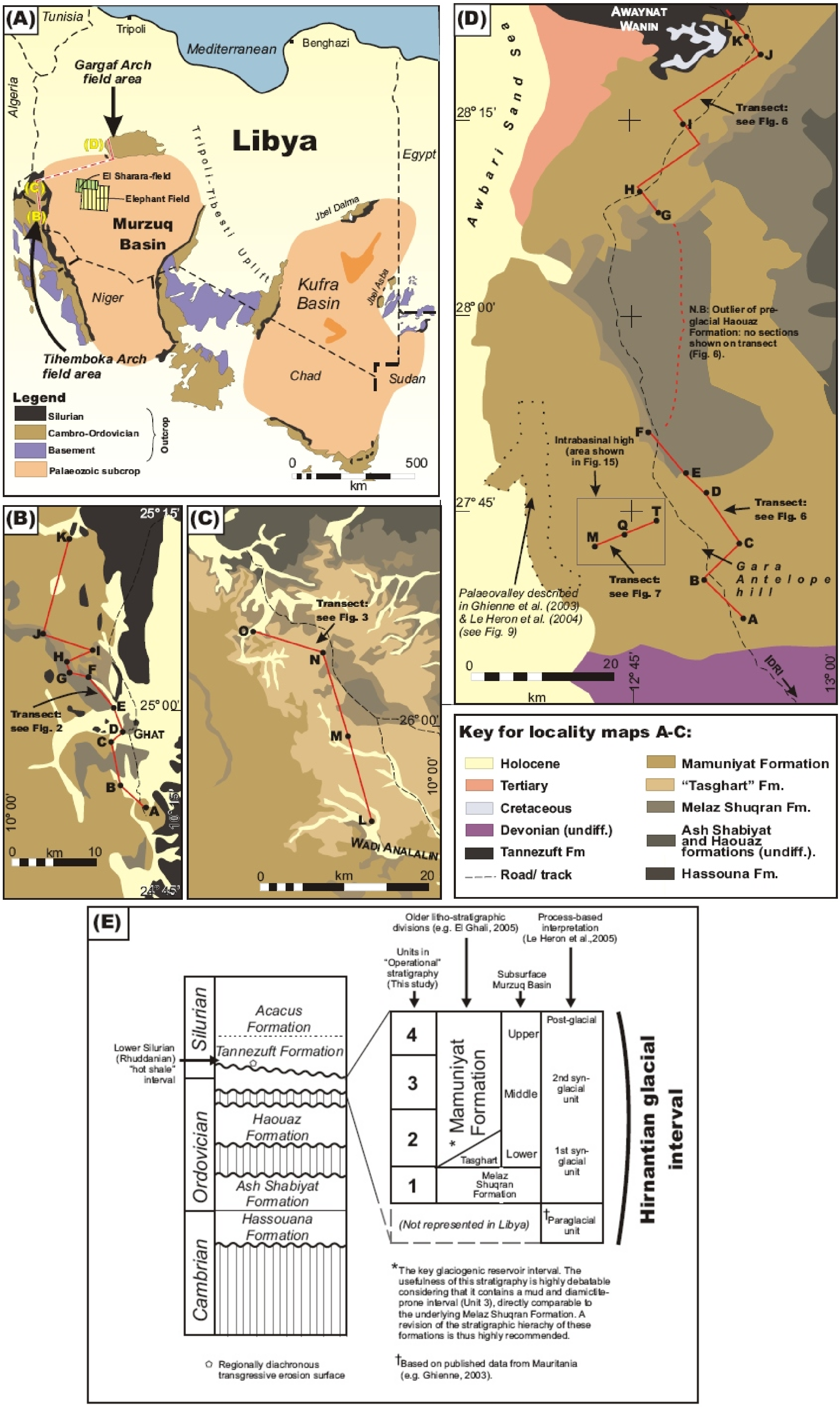
(A)
Tunisia
Tripoli
Mediterranean
Benghazi
Algeria
Gargaf Arch field area
Libya
Tripoli-Tibesti Uplift
Egypt
El Sharara-field
Elephant Field
Murzuq Basin
Jbel Dalma
Kufra Basin
Jbel Asba
Niger
Tihemboka Arch field area
Chad
Sudan
Legend
Silurian
Cambro-Ordovician
Basement
Palaeozoic subcrop
Outcrop
0 500 km
(B)
25° 15'
Transect: see Fig. 2
25° 00'
GHAT
10° 00'
10° 15'
24° 45'
0 km 10
(C)
Transect: see Fig. 3
26° 00'
10° 00'
WADI ANALALIN
0 km 20
(D)
AWAYNAT WANIN
Awbari Sand Sea
28° 15'
Transect: see Fig. 6
28° 00'
N.B: Outlier of pre-glacial Haouaz Formation: no sections shown on transect (Fig. 6).
Intrabasinal high (area shown in Fig. 15)
27° 45'
Transect: see Fig. 6
Gara Antelope hill
Transect: see Fig. 7
Palaeovalley described in Ghienne et al. (2003) & Le Heron et al. (2004) (see Fig. 9)
0 20 km
12° 45'
13° 00'
IDRI
Key for locality maps A-C:
Holocene
Tertiary
Cretaceous
Devonian (undiff.)
Tannezuft Fm
Road/ track
Mamuniyat Formation
"Tasghart" Fm.
Melaz Shuqran Fm.
Ash Shabiyat and Haouaz formations (undiff.).
Hassouna Fm.
(E)
Older litho-stratigraphic divisions (e.g. El Ghali, 2005)
Process-based interpretation (Le Heron et al., 2005)
Units in "Operational" stratigraphy (This study)
Subsurface Murzuq Basin
Silurian
Acacus Formation
Tannezuft Formation
Lower Silurian (Rhuddanian) "hot shale" interval
Ordovician
Haouaz Formation
Ash Shabiyat Formation
Hassouana Formation
Cambrian
4
3
2
1
* Mamuniyat Formation
Tasghart
Melaz Shuqran Formation
Upper
Middle
Lower
Post-glacial
2nd syn-glacial unit
1st syn-glacial unit
(Not represented in Libya)
†Paraglacial unit
Hirnantian glacial interval
*The key glaciogenic reservoir interval. The usefulness of this stratigraphy is highly debatable considering that it contains a mud and diamictite-prone interval (Unit 3), directly comparable to the underlying Melaz Shuqran Formation. A revision of the stratigraphic hierachy of these formations is thus highly recommended.
Regionally diachronous transgressive erosion surface
†Based on published data from Mauritania (e.g. Ghienne, 2003).

Figure 1

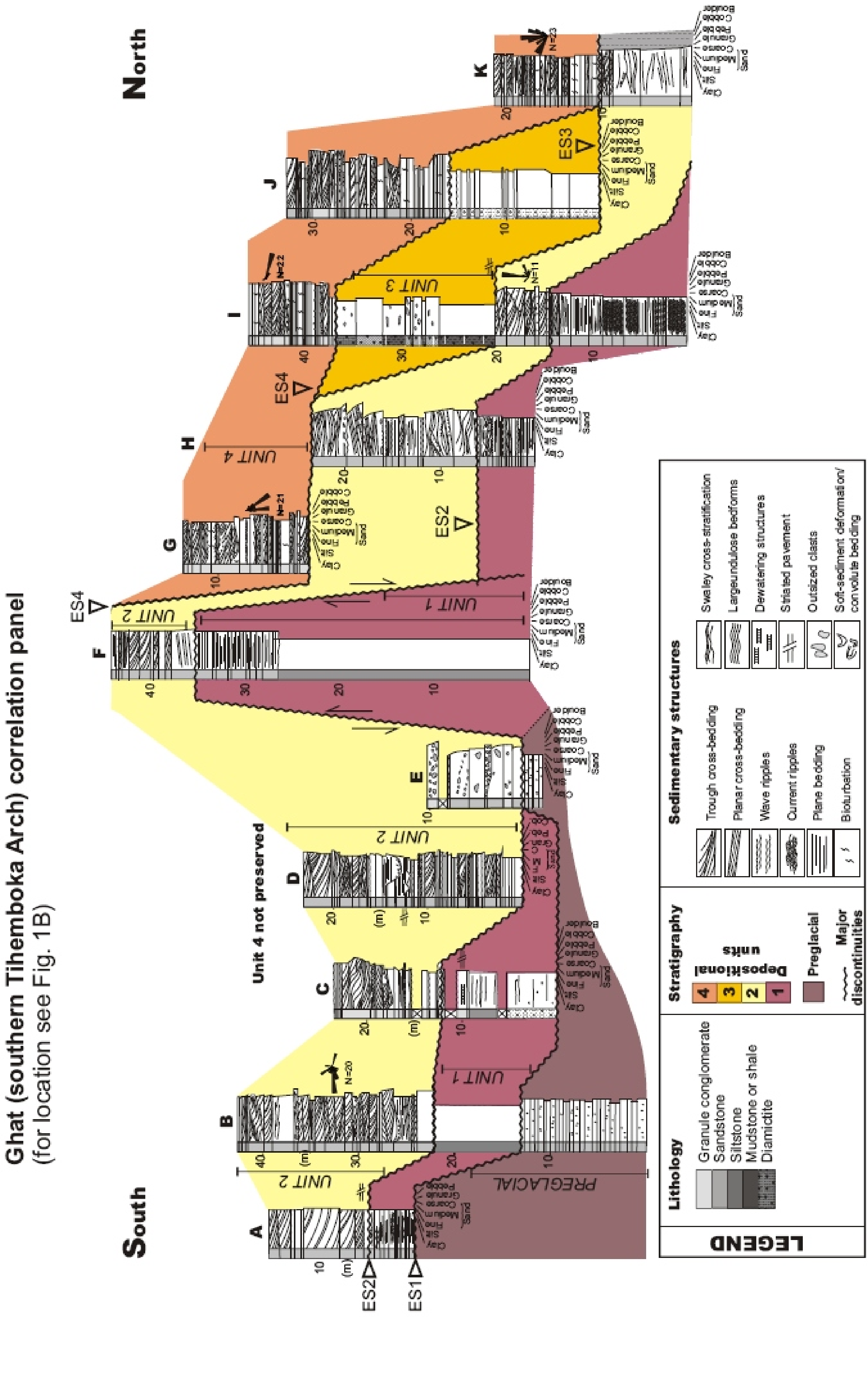

Ghat (southern Tihemboka Arch) correlation panel
(for location see Fig. 1B)
South
North
Unit 4 not preserved
UNIT 1
UNIT 2
UNIT 3
UNIT 4
PREGLACIAL
ES1
ES2
ES3
ES4
N=20
N=21
N=22
N=11
N=23
LEGEND
Lithology
Granule conglomerate
Sandstone
Siltstone
Mudstone or shale
Diamictite
Stratigraphy
Depositional units
Preglacial
Major discontinuities
Sedimentary structures
Trough cross-bedding
Planar cross-bedding
Wave ripples
Current ripples
Plane bedding
Bioturbation
Swaley cross-stratification
Largeundulose bedforms
Dewatering structures
Striated pavement
Outsized clasts
Soft-sediment deformation/ convolute bedding

Figure 2

Wadi Analalin (northern Tihemboka Arch) correlation panel
(for location see Fig. 1B)

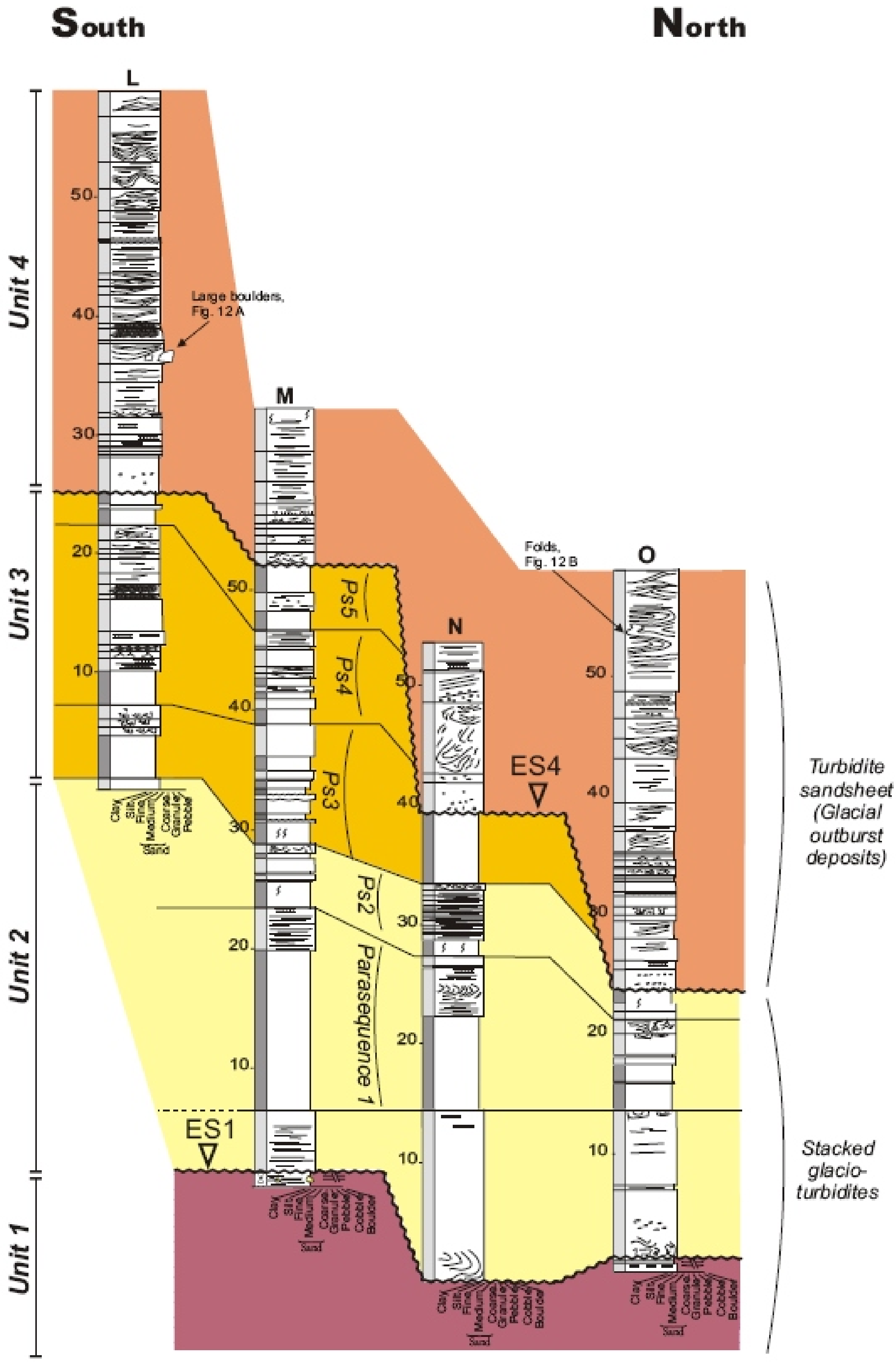

Figure 3

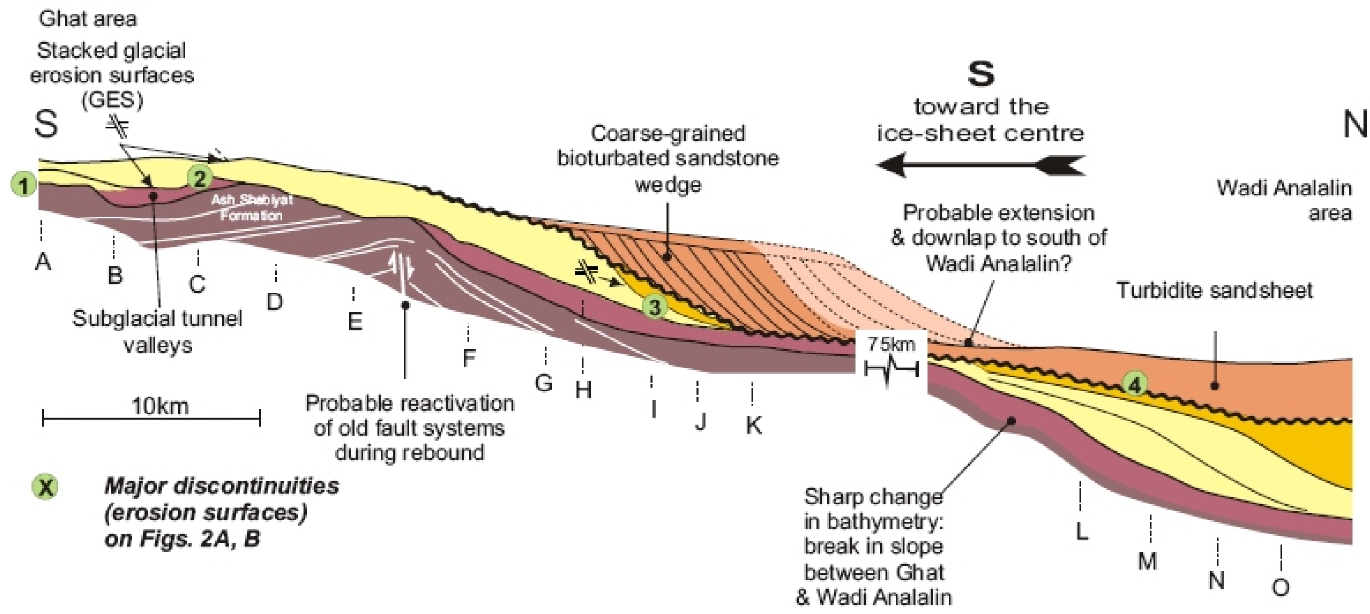
Ghat area
Stacked glacial erosion surfaces (GES)
S
1
2
Ash Shabiyat Formation
A
B
C
D
E
Subglacial tunnel valleys
10km
Probable reactivation of old fault systems during rebound
F
G
H
I
J
K
3
Coarse-grained bioturbated sandstone wedge
S
toward the ice-sheet centre
N
Wadi Analalin area
Probable extension & downlap to south of Wadi Analalin?
Turbidite sandsheet
75km
4
Sharp change in bathymetry: break in slope between Ghat & Wadi Analalin
L
M
N
O
X
Major discontinuities (erosion surfaces) on Figs. 2A, B

Figure 4

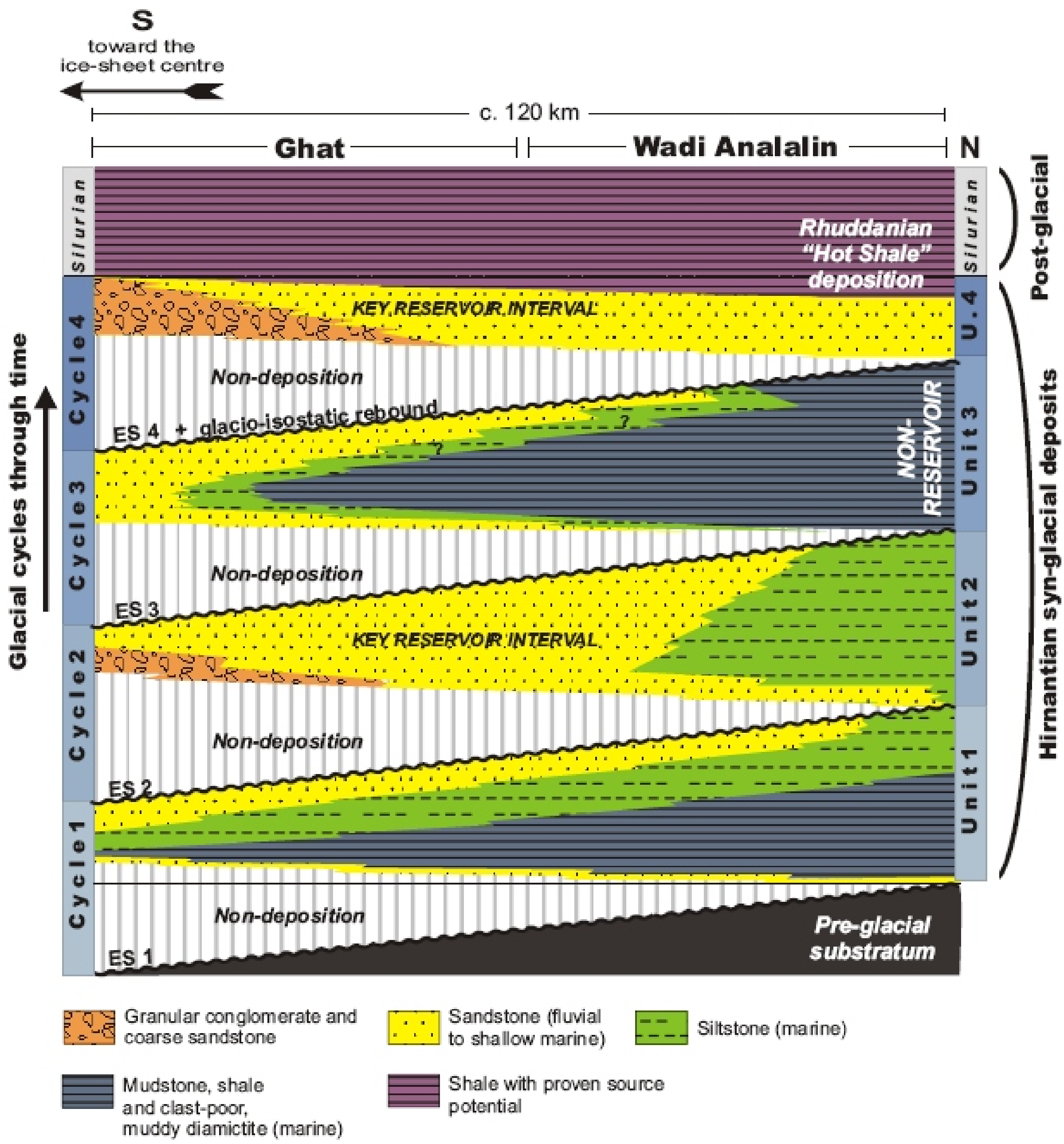

S
toward the ice-sheet centre
c. 120 km
Ghat
Wadi Analalin
N
Silurian
Rhuddanian "Hot Shale" deposition
Post-glacial
KEY RESERVOIR INTERVAL
Non-deposition
ES 4 + glacio-isostatic rebound
NON-RESERVOIR
ES 3
KEY RESERVOIR INTERVAL
Non-deposition
ES 2
Non-deposition
ES 1
Pre-glacial substratum
Cycle 1
Cycle 2
Cycle 3
Cycle 4
Glacial cycles through time
Unit 1
Unit 2
Unit 3
U. 4
Hirnantian syn-glacial deposits
Granular conglomerate and coarse sandstone
Sandstone (fluvial to shallow marine)
Siltstone (marine)
Mudstone, shale and clast-poor, muddy diamictite (marine)
Shale with proven source potential

Figure 5

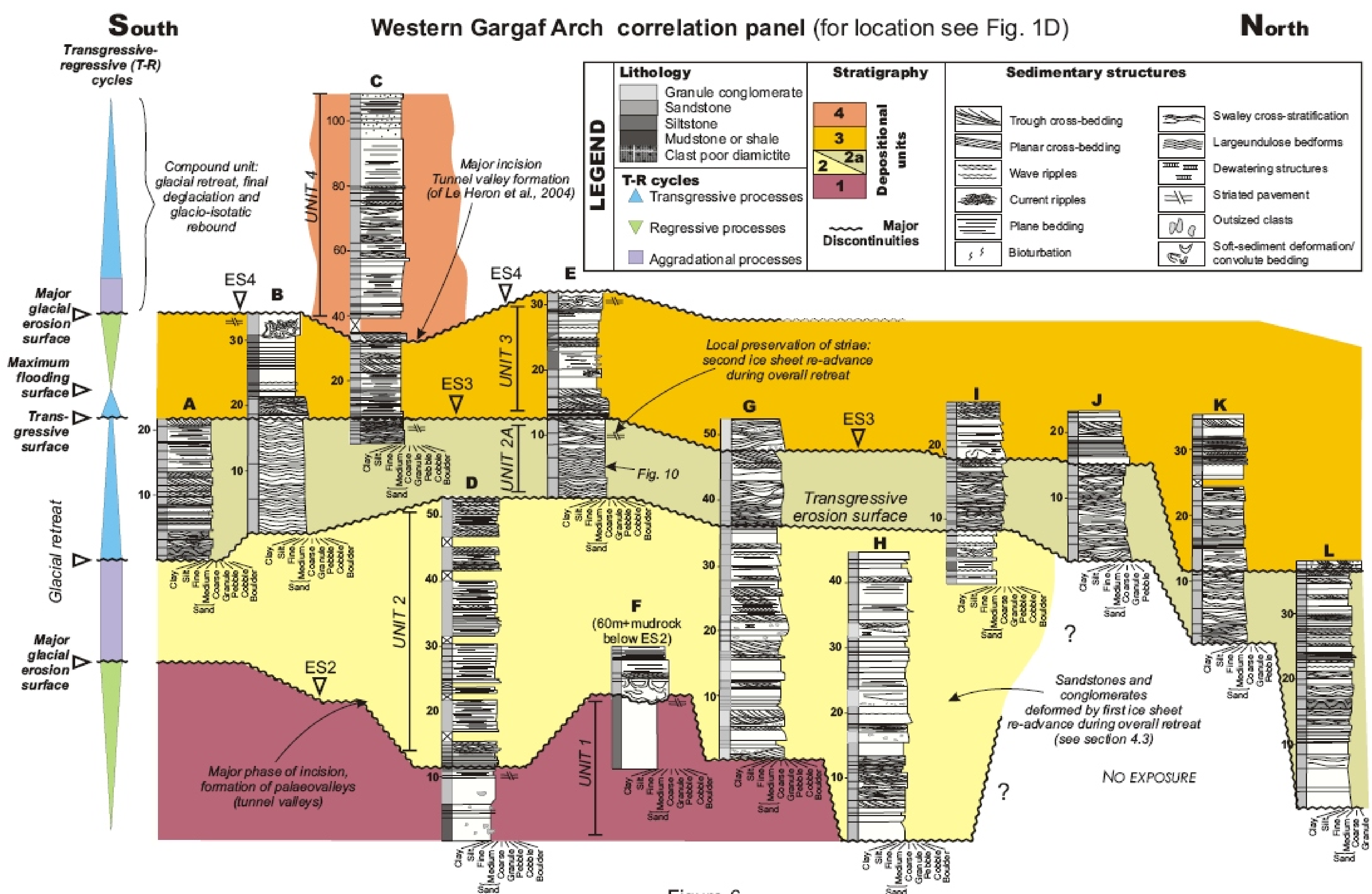
South
Western Gargaf Arch correlation panel (for location see Fig. 1D)
North
Transgressive-regressive (T-R) cycles
Compound unit: glacial retreat, final deglaciation and glacio-isotatic rebound
Major glacial erosion surface
Maximum flooding surface
Trans-gressive surface
Glacial retreat
Major glacial erosion surface
ES4
ES3
ES2
UNIT 4
UNIT 3
UNIT 2A
UNIT 2
UNIT 1
A
B
C
D
E
F
G
H
I
J
K
L
Major incision
Tunnel valley formation
(of Le Heron et al., 2004)
Local preservation of striae: second ice sheet re-advance during overall retreat
Fig. 10
Transgressive erosion surface
(60m+ mudrock below ES2)
Major phase of incision, formation of palaeovalleys (tunnel valleys)
Sandstones and conglomerates deformed by first ice sheet re-advance during overall retreat (see section 4.3)
NO EXPOSURE
Clay
Silt
Fine
Medium
Coarse
Sand
Granule
Pebble
Cobble
Boulder
LEGEND
Lithology
Granule conglomerate
Sandstone
Siltstone
Mudstone or shale
Clast poor diamictite
T-R cycles
Transgressive processes
Regressive processes
Aggradational processes
Stratigraphy
Depositional units
4
3
2
2a
1
Major Discontinuities
Sedimentary structures
Trough cross-bedding
Planar cross-bedding
Wave ripples
Current ripples
Plane bedding
Bioturbation
Swaley cross-stratification
Largeundulose bedforms
Dewatering structures
Striated pavement
Outsized clasts
Soft-sediment deformation/ convolute bedding

Figure 6

Gargaf Arch: correlation panel across intrabasinal high
(for location see Fig. 1D)

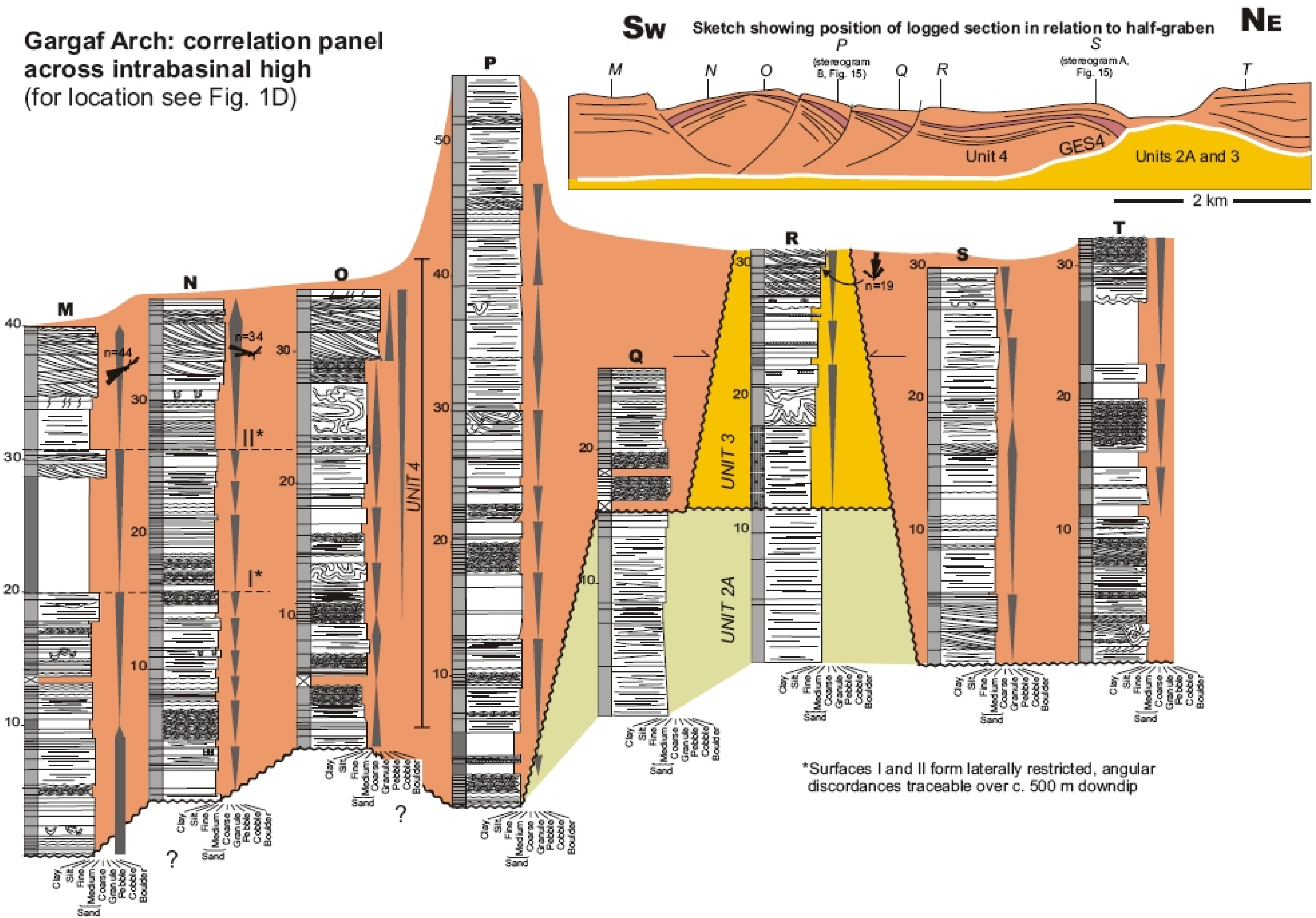

*Surfaces I and II form laterally restricted, angular discordances traceable over c. 500 m downdip

Figure 7

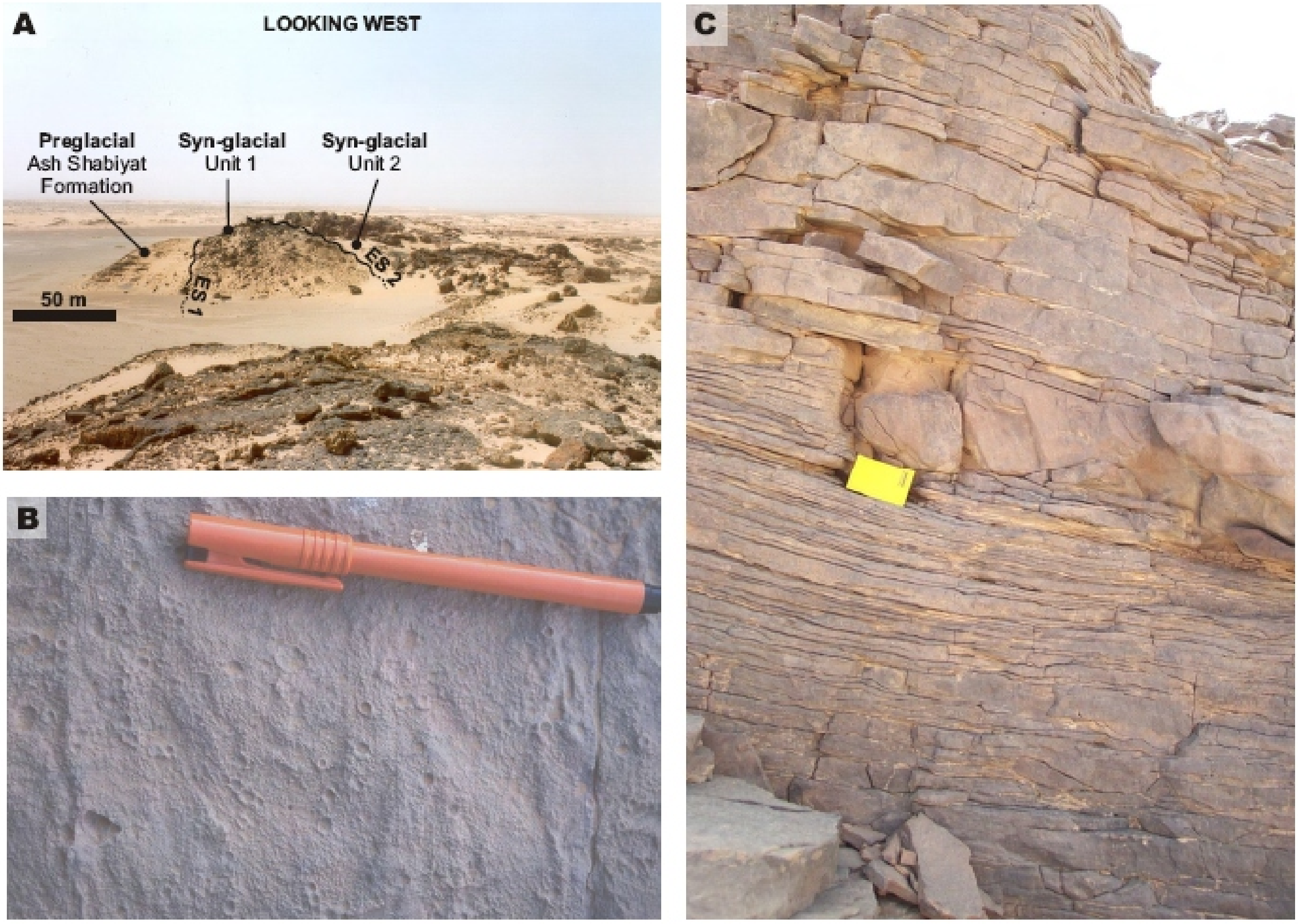
A
LOOKING WEST
Preglacial
Ash Shabiyat
Formation
Syn-glacial
Unit 1
Syn-glacial
Unit 2
ES 1
ES 2
50 m
B
C

Figure 8

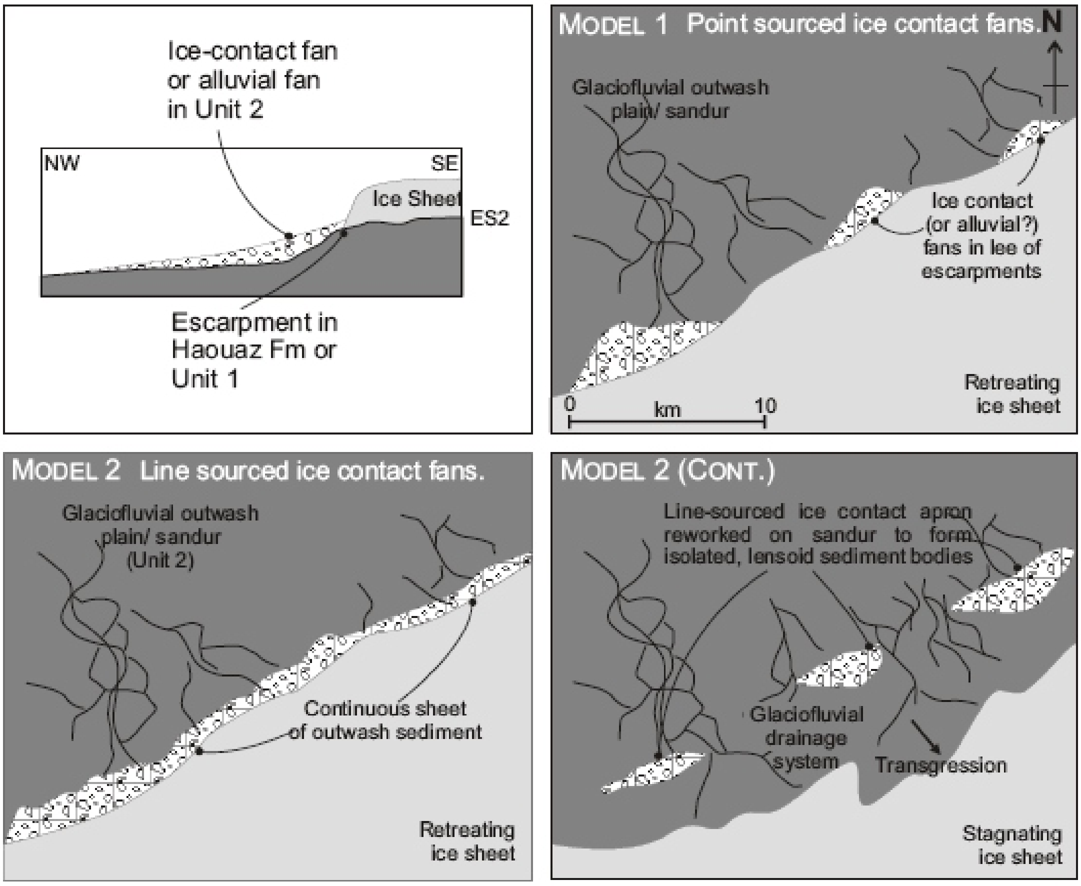
Ice-contact fan
or alluvial fan
in Unit 2
NW
SE
Ice Sheet
ES2
Escarpment in
Haouaz Fm or
Unit 1
MODEL 1 Point sourced ice contact fans.
N
Glaciofluvial outwash
plain/ sandur
Ice contact
(or alluvial?)
fans in lee of
escarpments
Retreating
ice sheet
0
km
10
MODEL 2 Line sourced ice contact fans.
Glaciofluvial outwash
plain/ sandur
(Unit 2)
Continuous sheet
of outwash sediment
Retreating
ice sheet
MODEL 2 (CONT.)
Line-sourced ice contact apron
reworked on sandur to form
isolated, lensoid sediment bodies
Glaciofluvial
drainage
system
Transgression
Stagnating
ice sheet

Figure 9

Figure 10

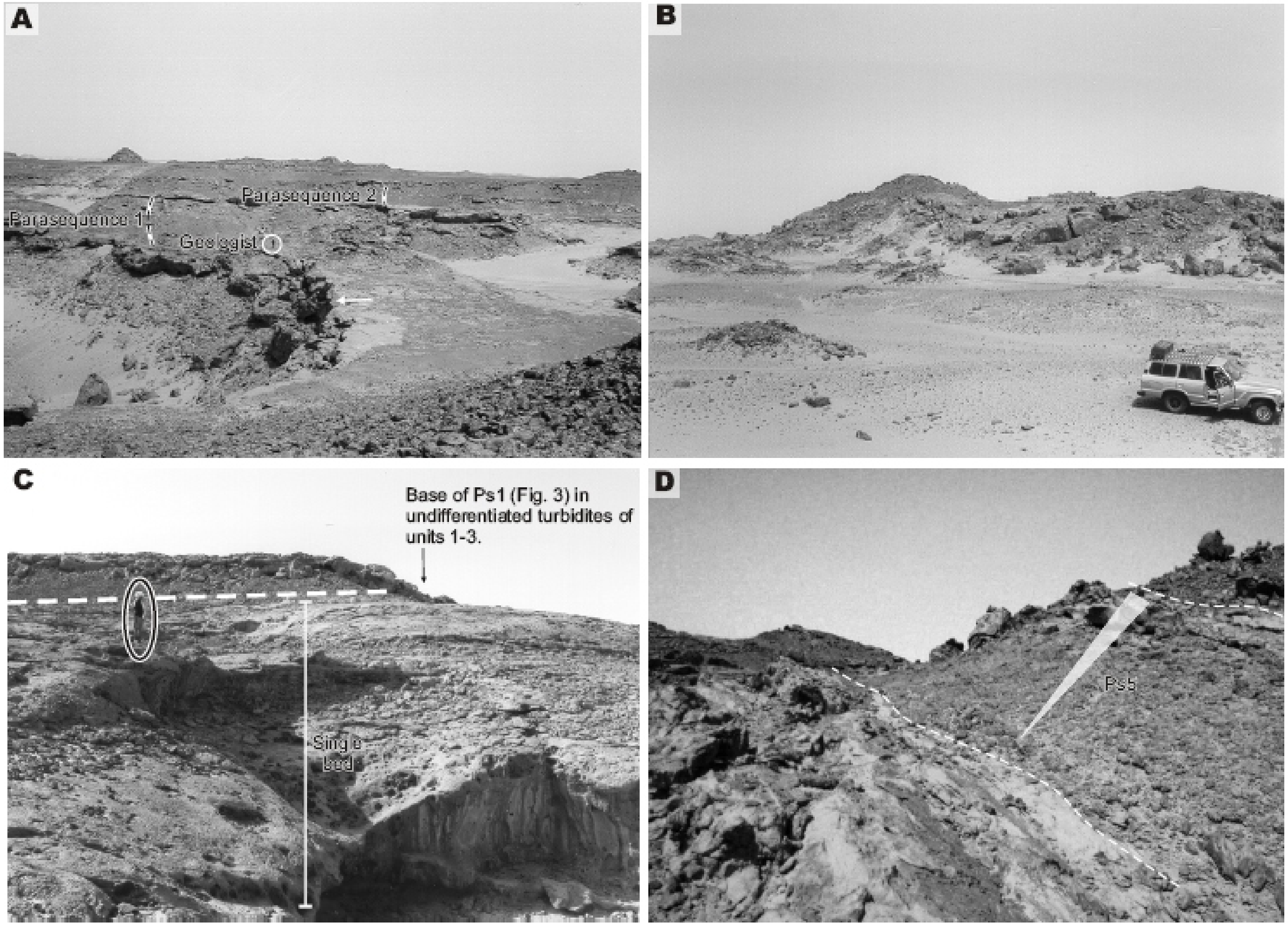
A
Parasequence 1
Parasequence 2
Geologist
B
C
Base of Ps1 (Fig. 3) in undifferentiated turbidites of units 1-3.
Single bed
D
Ps5

Figure 11

Figure 12

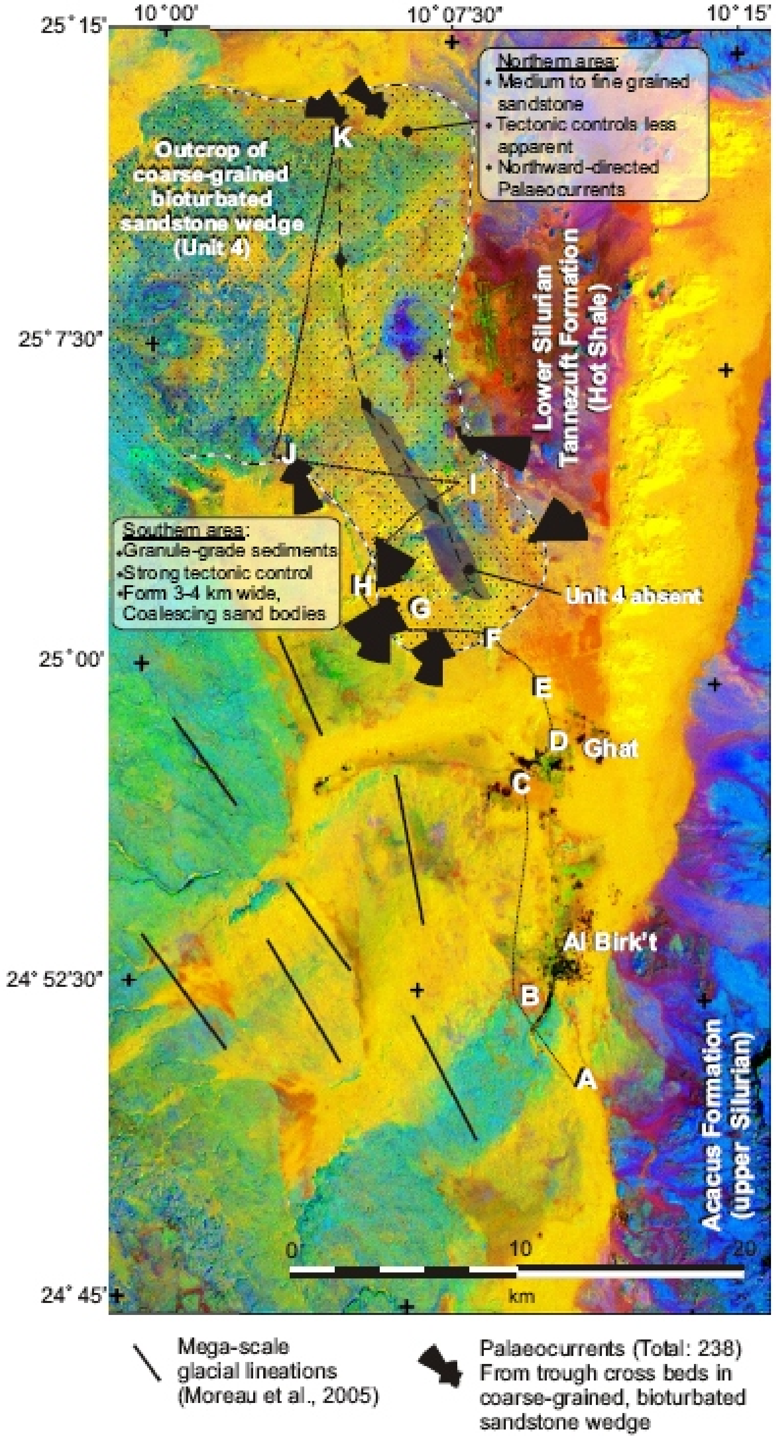

10°00'
10°07'30"
10°15'
25°15'
25°7'30"
25°00'
24°52'30"
24°45'
Northern area:
• Medium to fine grained sandstone
• Tectonic controls less apparent
• Northward-directed Palaeocurrents
Outcrop of coarse-grained bioturbated sandstone wedge (Unit 4)
Lower Silurian Tannezuft Formation (Hot Shale)
Southern area:
•Granule-grade sediments
•Strong tectonic control
•Form 3-4 km wide, Coalescing sand bodies
Unit 4 absent
K
J
I
H
G
F
E
D
C
B
A
Ghat
Al Birk't
Acacus Formation (upper Silurian)
0
10
20
km
Mega-scale glacial lineations (Moreau et al., 2005)
Palaeocurrents (Total: 238) From trough cross beds in coarse-grained, bioturbated sandstone wedge

Figure 13

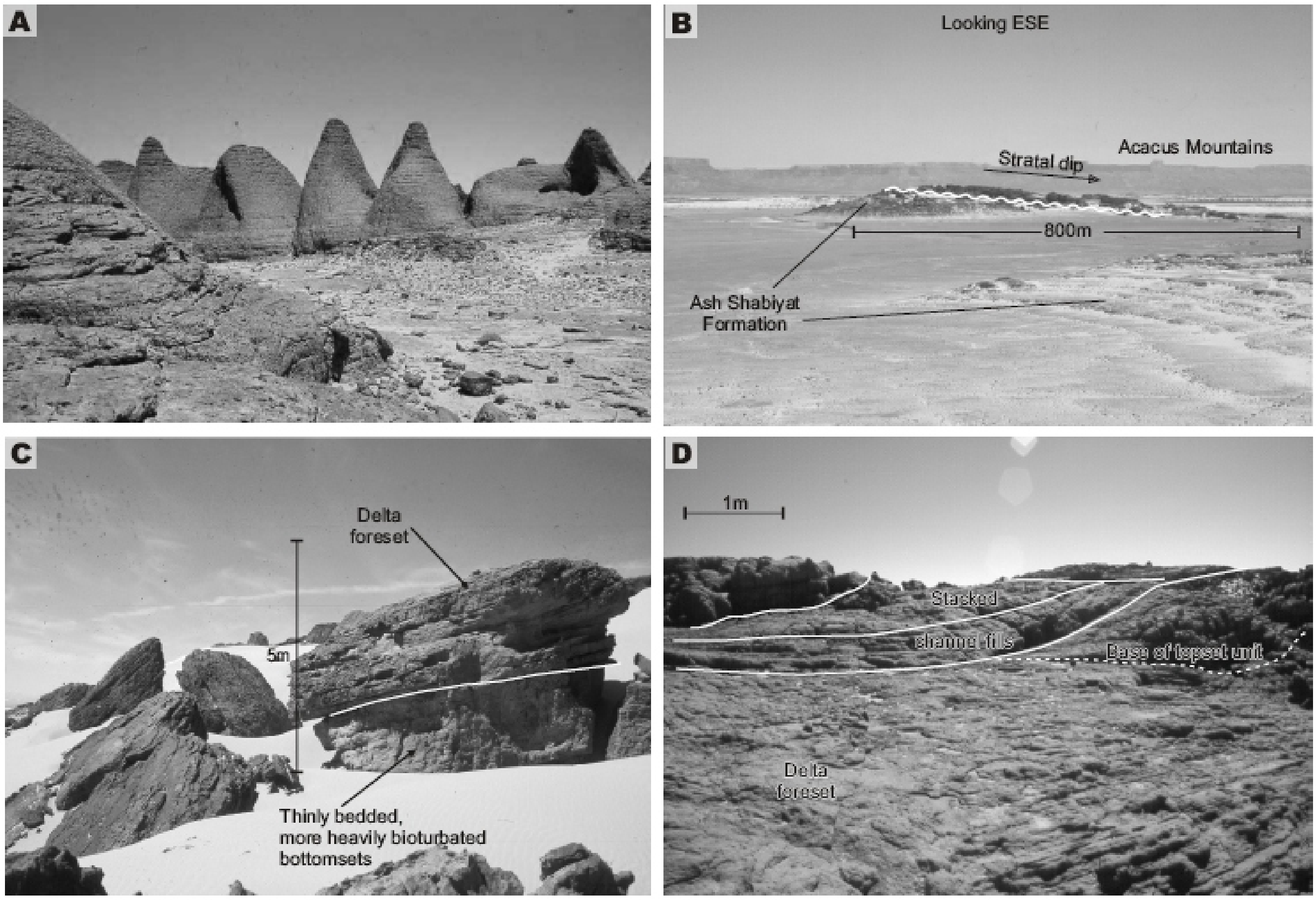
A
B
Looking ESE
Acacus Mountains
Stratal dip
800m
Ash Shabiyat
Formation
C
Delta
foreset
5m
Thinly bedded,
more heavily bioturbated
bottomsets
D
1m
Stacked
channel-fills
Base of topset unit
Delta
foreset

Figure 14

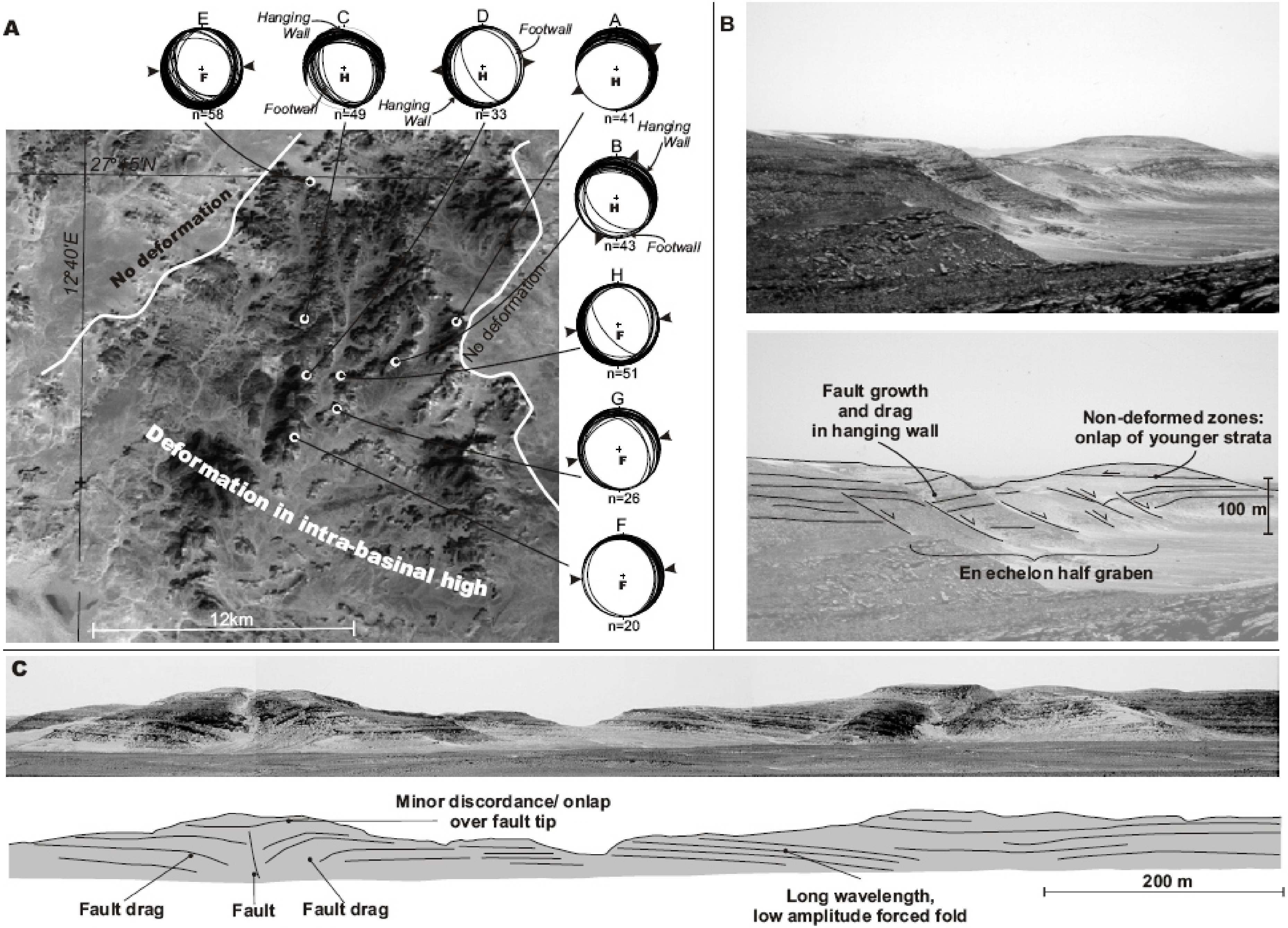
A
E
C
D
A
B
H
G
F
Hanging Wall
Footwall
n=58
n=49
n=33
n=41
n=43
n=51
n=26
n=20
27°15'N
12°40'E
No deformation
Deformation in intra-basinal high
12km
B
Fault growth and drag in hanging wall
Non-deformed zones: onlap of younger strata
100 m
En echelon half graben
C
Minor discordance/ onlap over fault tip
Fault drag
Fault
Fault drag
Long wavelength, low amplitude forced fold
200 m

Figure 15

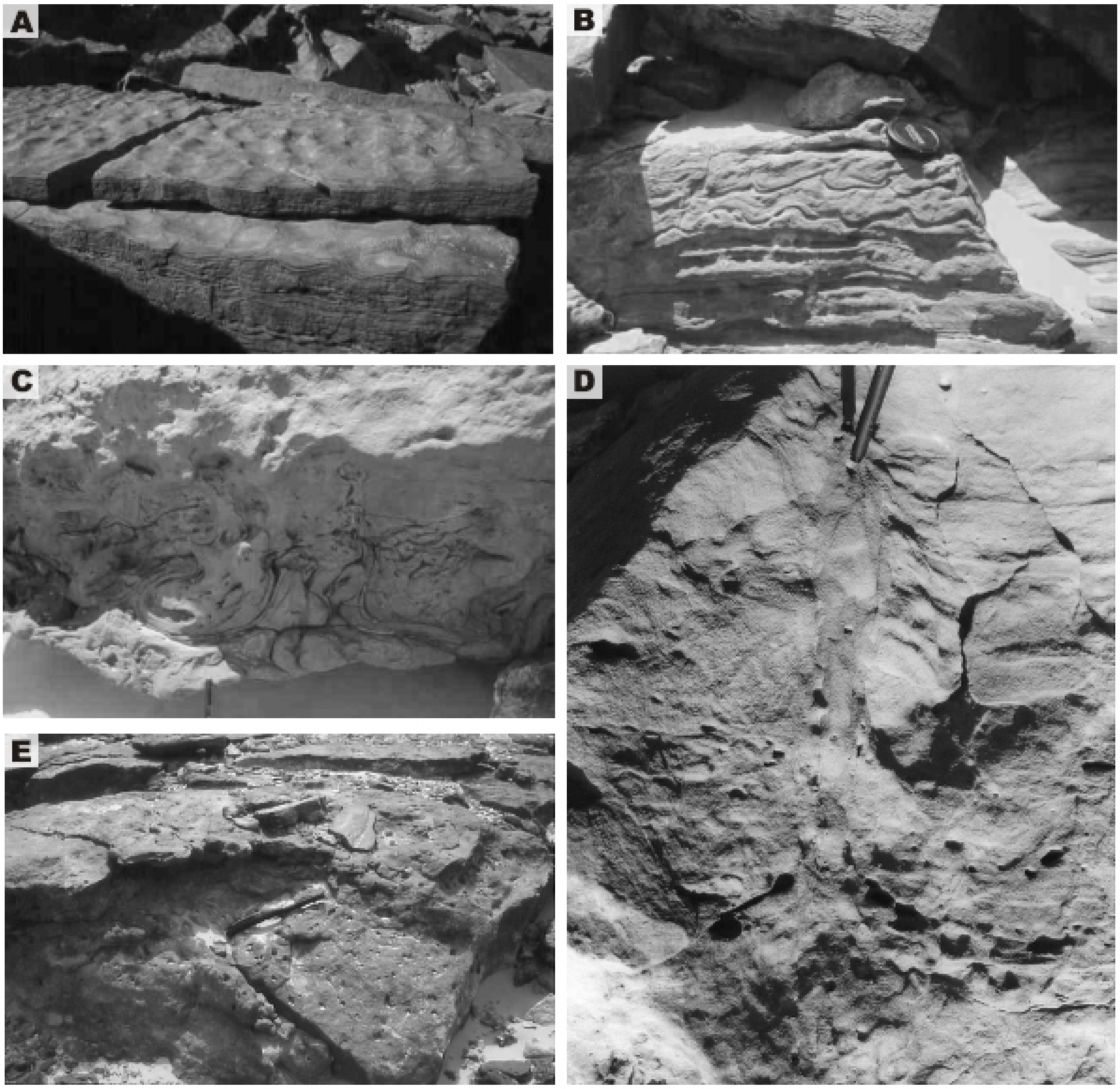

Figure 16

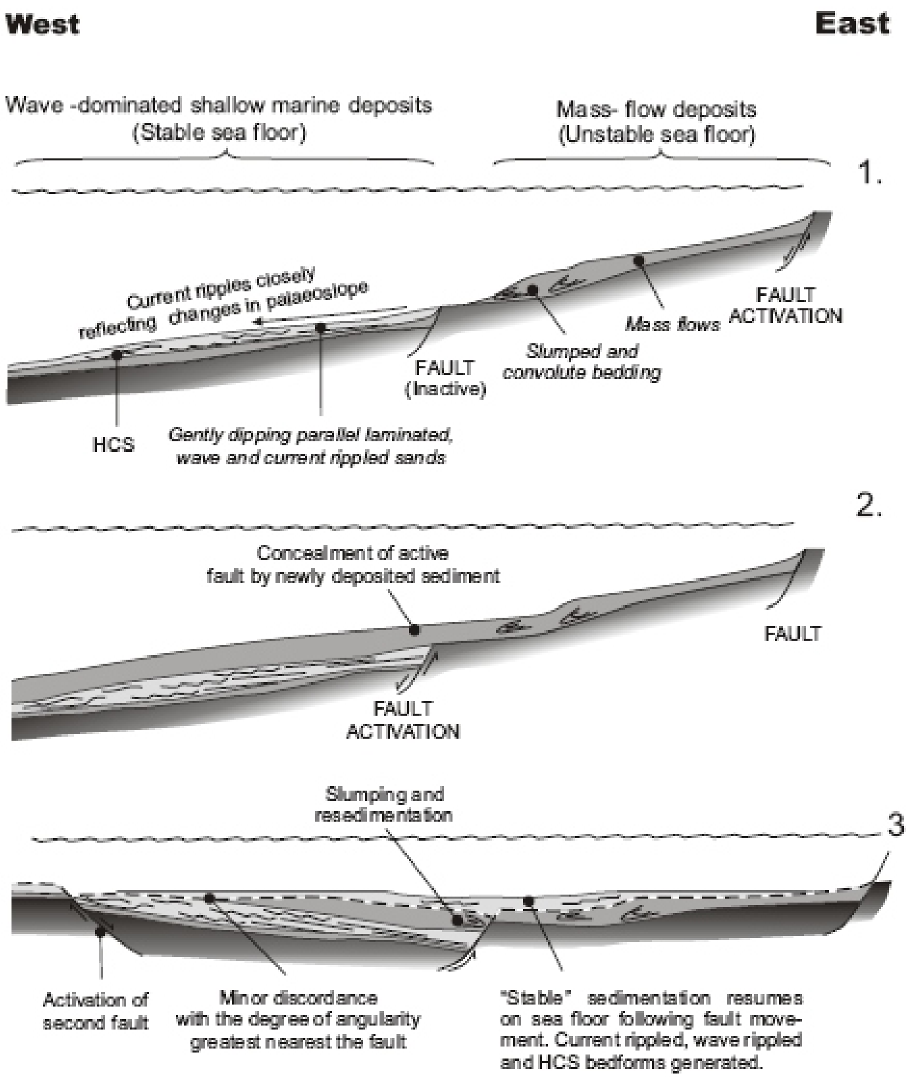

1. Mass-flow is triggered by normal fault activation. Shallow marine sedimentation continues away from the fault.

2. Mass flow continues basinward, and is possibly enhanced by continued movement along the fault.

3. Subsidence, possibly enhanced by movement of eastward - dipping faults results in angular discordance. Resultant subtle changes in gradient may explain rapid changes in current ripple orientation upsection.

Figure 17

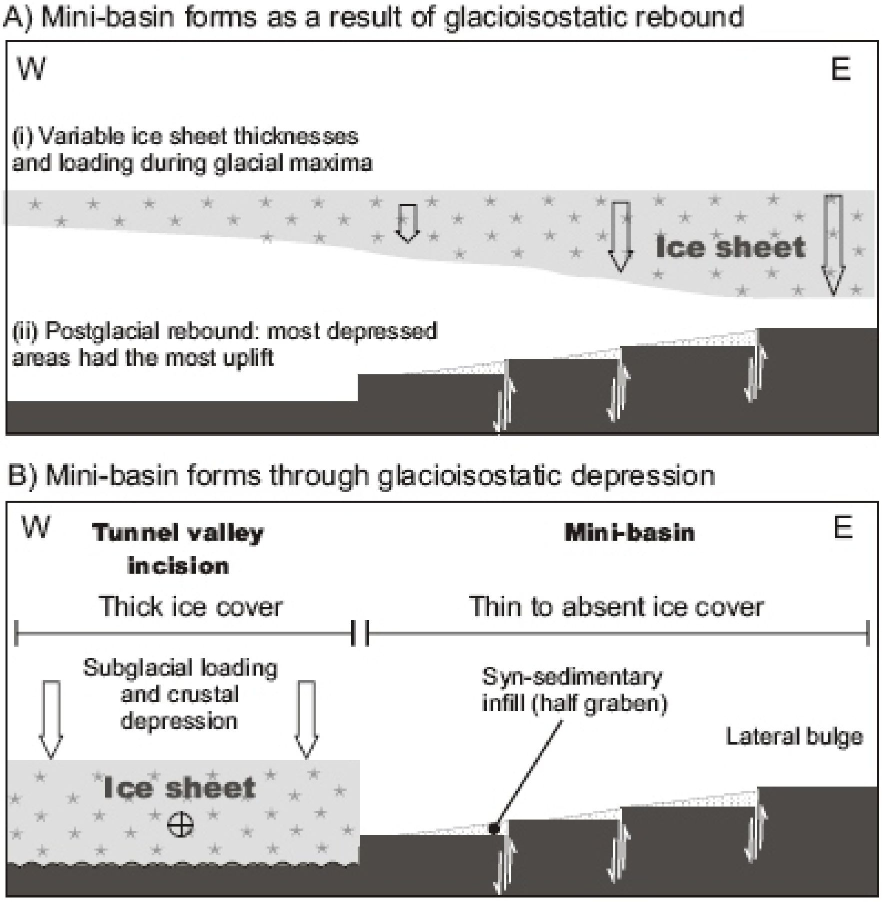
A) Mini-basin forms as a result of glacioisostatic rebound
W
E
(i) Variable ice sheet thicknesses and loading during glacial maxima
Ice sheet
(ii) Postglacial rebound: most depressed areas had the most uplift
B) Mini-basin forms through glacioisostatic depression
W
Tunnel valley incision
Mini-basin
E
Thick ice cover
Thin to absent ice cover
Subglacial loading and crustal depression
Syn-sedimentary infill (half graben)
Lateral bulge
Ice sheet

Figure 18